GeroScience (2022) 44:763–783
https://doi.org/10.1007/s11357-022-00527-1

ORIGINAL ARTICLE

Selective brain regional changes in lipid profile with human aging

Natalia Mota-Martorell · Pol Andrés-Benito · Meritxell Martín-Gari · José Daniel Galo-Licona · Joaquim Sol · Anna Fernández-Bernal · Manuel Portero-Otín · Isidro Ferrer · Mariona Jove · Reinald Pamplona

Received: 10 September 2021 / Accepted: 29 January 2022 / Published online: 11 February 2022

Abstract Fatty acids are key components in the structural diversity of lipids and play a strategic role in the functional properties of lipids which determine the integrity of neuronal and glial cell membranes, the generation of lipid signaling mediators, and the chemical reactivity of acyl chains. The present study analyzes using gas chromatography the fatty acid profiles of 13 regions of the human central nervous system in healthy individuals ranging from 40 to 80 years old. The outcomes suggest the existence of general traits in fatty acid composition such as an average chain length of 18 carbon atoms, high monounsaturated fatty acid content, and predominance in polyunsaturated fatty acids of those of series n-6 over series n-3 which are shared by all brain regions regardless of age. Our results also show a general sustained and relatively well-preserved lipid profile throughout the adult lifespan in most studied regions (olive, upper vermis, substantia nigra, thalamus, hippocampus, putamen, caudate, occipital cortex,

Supplementary Information The online version contains supplementary material available at https://doi.org/10.1007/s11357-022-00527-1.

N. Mota-Martorell · M. Martín-Gari · J. D. Galo-Licona · J. Sol · A. Fernández-Bernal · M. Portero-Otín · M. Jove (✉) · R. Pamplona (✉)
Department of Experimental Medicine, University of Lleida—Lleida Biomedical Research Institute (UdL-IRBLleida), 25198 Lleida, Spain
e-mail: mariona.jove@udl.cat

R. Pamplona
e-mail: reinald.pamplona@udl.cat

N. Mota-Martorell
e-mail: nataliamotamartorell@gmail.com

M. Martín-Gari
e-mail: meritxell.martin@udl.cat

J. D. Galo-Licona
e-mail: jgalolic25@gmail.com

J. Sol
e-mail: solcullere@gmail.com

A. Fernández-Bernal
e-mail: anna.fernandez@udl.cat

M. Portero-Otín
e-mail: manuel.portero@udl.cat

P. Andrés-Benito · I. Ferrer
Center for Biomedical Research On Neurodegenerative Diseases (CIBERNED), Institute of Health Carlos III, 28220 Madrid, Spain
e-mail: pol.andres.benito@gmail.com

I. Ferrer
e-mail: 8082ifa@gmail.com

I. Ferrer
Department of Pathology and Experimental Therapeutics, University of Barcelona, L'Hospitalet de Llobregat, 08907 Barcelona, Spain

I. Ferrer
Institute of Biomedical Research of Bellvitge (IDIBELL), 08907 Hospitalet de Llobregat, Spain

parietal cortex, entorhinal cortex, and frontal cortex) with minor changes that are region-dependent. In contrast, of particular relevance is the involvement of the inferior temporal cortex and cingulate cortex. It is proposed that during normal human brain aging, the lipid profile is resistant to changes with age in most human brain regions to ensure cell survival and function, but some particular regions involved in specific memory domains are greatly affected.

Keywords Average chain length · Cerebral cortex · Human brain regions · Fatty acid profile · Peroxidizability index · Polyunsaturated fatty acids

Introduction

Human brain evolution and lipids are closely linked [1, 2]. Structural and functional diversity and abundance of lipids are also traits of the human brain [1, 3–5]. As result, all lipid classes are present in the nervous system, likely as expression and support of the structural and functional complexity of the system [4, 6]. This abundance and diversity of lipids require a quarter of the total brain energy to maintain cellular activity involved in de novo lipid biosynthesis, remodeling, turnover, and synthesis of lipid-derived mediators, as well as continuous adjustment of the spatial and temporal lipid organization of cell membranes [7, 8].

Fatty acids are major components of glycerolipids, glycerophospholipids, and sphingolipids. The combination of fatty acids or fatty acids with different head groups (depending on the lipid class) can generate around 10,000 different lipid molecular species [6]. The length (number of carbon atoms) of the acyl chain and number of double bonds are determinants of the geometric traits of lipids influencing membrane organization and function [4]. Furthermore, fatty acids are substrates for the generation of lipid signaling mediators [9]. An additional trait assigned to fatty acids is their chemical reactivity in the face of oxidative conditions [10], which, by extension, determines the susceptibility to oxidative stress for a given membrane [10]. Thus, polyunsaturated side chains are much more easily attacked by oxidant agents than saturated or monounsaturated fatty acid side chains.

In this context, it has been suggested that the morphological and functional diversity among neural cells in the human brain is also achieved by the expression of region-specific lipid profiles [10]. In agreement with this hypothesis, we recently demonstrated that particular fatty acids are significant discriminators among human brain regions and that these specific fatty acid profiles generate a differential cross-regional selective neural vulnerability (expressed by the double bond index and peroxidizability index). In other words, there is a region-specific vulnerability to lipid peroxidation in human brain [10]. Changes in global lipid composition have been reported in human brain aging, and in several age-associated neurodegenerative diseases such as Alzheimer disease [5]. However, little is known about alterations occurring across brain regions throughout the adult human lifespan.

The present study analyzes the fatty acid profiles of total lipids from the gray matter of 13 different regions of the human central nervous system belonging to the hindbrain (*olive* and *upper vermis*), midbrain (*substantia nigra*), diencephalon (*thalamus*), subcortical telencephalon (*hippocampus*, *head of the caudate*, and *anterior putamen*), and cortical telencephalon (*occipital cortex areas 17–18*, *parietal cortex area 7*, *inferior temporal cortex area 20*, *entorhinal cortex*, *frontal cortex area 8*, and *cingulate gyrus area 24*), in healthy individuals without co-morbidities ranging from 40 to 80 years old. The brain areas were selected on the basis of their selective vulnerability to neurodegenerative diseases in aging. Our results show selective brain regional changes in lipid profile with human healthy aging.

Material and methods

Chemicals

Unless otherwise specified, all reagents were from Sigma-Aldrich and were of the highest purity available.

Human samples

Brain samples were obtained from the Institute of Neuropathology Brain Bank, a branch of the HUB-ICO-IDIBELL Biobank, following the guidelines of Spanish legislation (Real Decreto 1716/2011) and the approval of the local ethics committee (CEIC/1981).

At autopsy, one hemisphere was fixed in 4% buffered formalin for about 3 weeks while the other hemisphere was cut in coronal Sects. 0.5-cm thick; selected areas of the brain were dissected, immediately frozen on metal plates over dry ice, placed in labelled plastic bags, and stored at – 80 °C until use. Procedures were designed to preserve post-mortem material under optimal conditions for morphological and biochemical studies [11]. The post-mortem delay ranged from 2 to 14 h 40 min (see Table 1).

The neuropathological study, to discriminate healthy brains, was carried out in every case as previously described [11]. Briefly, the neuropathological study was carried out on formalin-fixed, paraffin-embedded samples of 26 brain regions. De-waxed sections, 4-µm thick, were stained with hematoxylin and eosin, and Klüver Barrera, or processed for immunohistochemistry to β-amyloid, phosphorylated tau (including clone AT8), α-synuclein, ubiquitin, p62, TDP43, glial fibrillary protein, and microglia markers.

Adult and middle-aged individuals (< 60 years) had no clinical or neuropathological alterations, whereas old-aged individuals (> 60 years) had no clinical symptoms and neuropathological alteration restricted to stage I of neurofibrillary degeneration. Since the majority of human beings aged 65 years have stages I–II of neurofibrillary tangle pathology [12, 13], the old-aged group was considered representative of normal brain aging. β-Amyloid deposition was absent in every case. All cases included in this study were without co-morbidities. Samples were from individuals with no neurological symptoms and without systemic and focal infectious or inflammatory and autoimmune diseases. Cases with disseminated malignant diseases, metabolic syndrome, or drug abuse (for instance, excessive ethanol consumption) were not included. Special care was also taken to not include cases with prolonged agonal state (patients subjected to intensive care or experiencing hypoxia). After neuropathological examination, cases with both neurodegenerative and vascular diseases were excluded excepting those with stages I–II of neurofibrillary tangle pathology. Finally, cases with associated neurodegenerative processes (i.e., TDP-43 proteinopathy, argyrophilic grain pathology, α-synucleinopathy, and other tauopathies) were also excluded.

Following initial screening, the present series included 17 cases: 12 males and 5 females, with age ranging from 40 to 80 years. Table 1 summarizes cases examined in the present series. The gray matter from cerebral cortex (frontal area 8, parietal area 7, inferior temporal area 20, occipital areas 17–18, cingulate gyrus area 24, entorhinal cortex, and hippocampus), striatum (head of the caudate and anterior

Table 1 Summary of cases examined

Case	Gender	Age (years)	Post-mortem delay	Neuropathology	Cause of death
1	Male	40	5 h 10 min	NL	CA
2	Female	40	8 h 45 min	NL	PNEU
3	Male	44	6 h 40 min	NL	THR-EMB
4	Male	45	4 h 5 min	CRIB	C-INF
5	Female	46	7 h 15 min	CRIB	MYO
6	Female	48	4 h 5 min	NL	CA
7	Male	52	9 h 30 min	NL	PNEU
8	Male	52	4 h 40 min	NL	C-INF
9	Male	57	5 h 20 min	NL	PNEU
10	Male	61	4 h 30 min	I-II	CA
11	Male	66	6 h 25 min	I-II	THR-EMB
12	Male	67	14 h 40 min	I-II	CA
13	Male	70	2 h 00 min	I-II	CA
14	Female	75	6 h 10 min	I-II + CRIB	C-INF
15	Male	76	6 h 30 min	I-II	PNEU
16	Male	77	6 h 55 min	I-II + CRIB	C-INF
17	Female	79	6 h 25 min	I-II + CRIB	INT-INF

NL, no lesions; *CRIB*, status cribosus; *I-II*, neurofibrillary tangle pathology stages I–II of Braak and Braak; *CA*, carcinoma; *PNEU*, pneumonia; *C-INF*, cardiac infarction; *THR-EMB*, pulmonary thrombosis-embolism; *MYO*, myocardiopathy; *INT-INF*, intestinal infarction

putamen), thalamus, substantia nigra, upper vermis, and olive were dissected and used for biochemical studies.

Fatty acid profile

Fatty acyl groups of total lipids from gray matter of 13 human brain regions were analyzed as methyl ester derivatives (FAMEs) by gas chromatography (GC) as previously described [10, 14]. Firstly, 50 mg of tissue samples was homogenized in a buffer containing 180 mM KCl, 5 mM MOPS, 2 mM EDTA, 1 mM diethylenetriaminepentaacetic acid, and 1 µM butylated hydroxytoluene. Tissue samples were randomized prior to lipid extraction. Quality control samples were included at a ratio of 1:10. Then, total lipids from human brain homogenates were extracted with chloroform:methanol 2:1 (v/v). The chloroform phase was separated and evaporated under N_2, and the fatty acyl groups were transesterified by incubation in 2.5 ml of 5% methanolic HCl at 75 °C for 90 min. The resulting fatty acid methyl esters were extracted by adding 1 ml of saturated NaCl solution and 2.5 ml of *n*-pentane. Finally, the n-pentane phase was separated, evaporated under N_2, and redissolved in 75 µl of carbon disulfide. Two microliters was used for GC analysis.

Separation was performed with a DBWAX capillary column (30 m × 0.25 mm × 0.25 µm) in a GC System 7890A with a Series Injector 7683B and a FID detector (Agilent Technologies, Barcelona, Spain). Sample injection was in the splitless mode. The injection port was maintained at 250 °C, and the detector at 250 °C. The temperature program was 5 min at 145 °C, then 2 °C/min to 245 °C, and finally hold at 245 °C for 10 min, with a post-run at 250 °C for 10 min. So, total run time was 65 min, with a post-run time of 10 min. Identification of fatty acid methyl esters was made by comparison with authentic standards (Larodan Fine Chemicals, Malmö, Sweden) using a specific software of data analysis for GC from Agilent (OpenLAB CDS ChemStation v. C.01.10; Agilent Technologies, Barcelona, Spain) and subsequent revision and confirmation by an expert. Results are expressed as mol%.

The following fatty acyl indices were also calculated: saturated fatty acids (SFA); unsaturated fatty acids (UFA); ratio SFA/UFA; monounsaturated fatty acids (MUFA); polyunsaturated fatty acids (PUFA) from n-3 and n-6 series (PUFAn-3 and PUFAn-6); and average chain length (ACL)=[(Σ% Total14×14)+(Σ% Total16×16)+(Σ% Total18×18)+(Σ% Total20×20)+(Σ% Total22×22)+(Σ% Total24×24)]/100. The density of double bonds in the membrane was calculated with the double bond index, DBI=[(1×Σmol% monoenoic)+(2×Σmol% dienoic)+(3×Σmol% trienoic)+(4×Σmol% tetraenoic)+(5×Σmol% pentaenoic)+(6×Σmol% hexaenoic)]. Membrane susceptibility to peroxidation was calculated with the peroxidizability index, PI=[(0.025×Σmol% monoenoic)+(1×Σmol% dienoic)+(2×Σmol% trienoic)+(4×Σmol% tetraenoic)+(6×Σmol% pentaenoic)+(8×Σmol% hexaenoic)].

Elongase and desaturase activity was estimated from specific product/substrate ratios. For desaturase activity: D9D (n-7) = 16:1n-7/16:0; D9D (n-9) = 18:1n-9/18:0; D5D (n-6) = 20:4n-6/20:3n-6; D6D (n-3) (a) = 18:4n-3/18:3n-3; D6D (n-3) (b) = 24:6n-3/24:5n-3. For elongase activity: Elovl3 (n-9) (a) = 20:1n-9/18:1n-9; Elovl3 (n-9) (b) = 22:1n-9/20:1n-9; Elovl3 (n-9) (c) = 24:1n-9/22:1n-9;Elovl6 = 18:0/16:0; Elovl1-3–7 (a) = 20:0/18:0; Elovl1-3–7 (b) = 22:0/20:0; Elovl1-3–7 (c) = 24:0/22:0; Elovl 5(n-6) = 20:2n-6/18:2n-6; Elovl2-5 (n-6) = 22:4n-6/20:4n-6; Elovl 2–5(n-3) = 22:5n-3/20:5n-3, and Elovl 2(n-3) = 24:5n-3/22:5n-3. Finally, peroxisomal β-oxidation (PβOx) was estimated according to the ratio 22:6n-3/24:6n-3.

Statistics

Data were expressed as mean values ± SEM. Student's *t*-test was used to evaluate differences between age groups. Spearman's rank correlation was employed to assess possible relations for variables with age. Statistical significance was adjusted for multiple testing by controlling the false discovery rate according to the Benjamini–Hochberg method using a maximum discovery rate of 10%. Graphs were made and *t*-tests performed using GraphPad prism 8.0.1. Spearman correlation was made using IBM SPSS Statistics (v24.0.0.0). Spearman correlation matrix was constructed using RStudio (v1.3.1073). Functions used were included in the packages *corrplot* [15] and *Hmisc* [16]. *p* values inferior to 0.05 were considered statistically significant.

Results

General traits shared by human brain regions

The changes in brain fatty acid profile along the aging process were assessed by analyzing 25 different fatty acid species across 13 different brain regions, including the olive (medulla oblongata) and vermis (cerebellum) (hindbrain); substantia nigra (midbrain); thalamus (diencephalon); hippocampus, caudate, and putamen (subcortical telencephalon); and occipital, parietal, temporal, entorhinal, frontal, and cingulate cortex (cortical telencephalon). Results revealed that 16:0, 18:0, and 18:1n-9 are the most abundant fatty acids in human healthy brain, in both the middle-aged and the elderly, accounting for approximately 60% of global fatty acid composition (Table 2). In addition, specific enrichment of 20:4n-6 and 22:6n-3 is found in all regions. As a result, the average chain length (ACL) is maintained at around 18 carbon atoms, with a predominant presence of monounsaturated fatty acids (MUFA), followed by polyunsaturated fatty acids (PUFA), showing a higher relative abundance of PUFAn-6 with respect to PUFAn-3.

Brain regional changes in fatty acid profile: comparison of middle-aged and elderly groups

Comparison of middle-aged and elderly groups throughout the different brain regions analyzed verified the existence of minor changes (Table 2). Thus, in hindbrain, *olive* showed a decrease in 14:0 (30%, $p<0.05$) and increase in 22:5n-3 (30%, $p<0.05$) and 24:6n-3 (25%, $p<0.05$), fatty acids with a very low abundance, and no involvement in general indexes in the elderly group compared to the middle-aged group, whilst *vermis* only showed an increase in 20:0 (22%, $p<0.01$) in the elderly group, without any additional change. In the midbrain, and in a similar way to hindbrain, *substantia nigra* only showed an increase in 16:1n-7 (10%, $p<0.05$), and the very minor fatty acids 18:4n-3 (100%, $p<0.05$) and 24:0 (280%, $p<0.01$), as well as SFA content (3%, $p<0.05$), and a decrease in ACL (0.5%, $p<0.01$) and UFA (3%, $p<0.05$).

In diencephalon, *thalamus* showed a decrease in 22:4n-6 (17%, $p<0.05$) content and ACL (0.5%, $p<0.05$), and an increase in 24:5n-3 (40%, $p<0.05$) content in the elderly group compared to the middle-aged group. In subcortical telencephalon, the three analyzed regions, hippocampus, caudate, and putamen, also showed minor changes in the elderly group. Thus, in *hippocampus*, we only found a decrease in the relative abundance of fatty acids 22:1n-9 (35%, $p<0.05$) and 22:4n-6 (7%, $p<0.05$); in *caudate nucleus* a decrease in 18:3n-3 (30%, $p<0.05$), 24:0 (47%, $p<0.05$), and 24:6n-3 (36%, $p<0.05$), and an increase in the content of 20:0 (17%, $p<0.01$) and 20:4n-6 (13%, $p<0.05$); and in the *putamen nucleus*, a decrease in 22:4n-6 (13%, $p<0.01$), 22:5n-6 (30%, $p<0.05$), and PUFAn-6 (6%, $p<0.01$) contents, as well as ACL (0.5%, $p<0.01$).

Finally, six regions from human cerebral cortex (cortical telencephalon) were analyzed, again showing minor changes in the elderly group. Thus, in *occipital cortex* (areas 17–18), fatty acid composition analysis revealed a slight increase in the ACL (0.3%, $p<0.05$) in the elderly group compared to the middle-aged group; in *parietal cortex* (area 7), a decrease in 14:0 (17%, $p<0.05$) content, and increase in PUFAn-3 (15%, $p<0.05$) and DBI (6%, $p<0.05$) was observed; in *temporal cortex* (inferior temporal area 20), a decrease in 22:4n-6 (9%, $p<0.05$), 22:5n-6 (31%, $p<0.05$), 24:5n-3 (33%, $p<0.05$), 24:6n-3 (53%, $p<0.01$), and PUFAn-6 (9%, $p<0.05$), and an increase in 20:0 (12%, $p<0.05$) and estimation of the peroxisomal β-oxidation activity (123%, $p<0.001$) was detected; in *entorhinal cortex*, the only observed change was a decrease in PUFAn-6 content (7%, $p<0.05$); in *frontal cortex* (area 8), no change was verified; and finally, in *cingulate cortex* (area 24), only a slight increase in 20:0 (15%, $p<0.01$) was revealed.

Because of the large number of tests, adjustment for multiple comparisons was assessed using the Benjamini–Hochberg false discovery rate (FDR) analysis. p values when comparing the two groups of cases is shown in Table 2. As a result, only 24:0 and ACL in substantia nigra, and 24:6n-3 and peroxisomal β-oxidation in the temporal cortex were sustained following multiple comparison adjustment.

Brain regional changes in estimated desaturase and elongase activity: general traits

Since some of the observed changes in the elderly group may be due to alterations in the activity of the enzymes involved in the fatty acid biosynthesis,

Table 2 Fatty acid composition of total lipids from different human brain regions comparing middle-aged and elderly individuals. Healthy individuals were grouped as middle-aged (<60 years) and elderly (>60 years). Differences between groups were assessed by applying a *t*-test and corrected by FDR method of Benjamini and Hochberg, with $Q = 10\%$. Values are reported in mol% as mean ± SEM from 8 to 9 individuals × group. $P < 0.05$ was selected as the minimum level of statistical significance. Significance compared to middle-aged group prior FDR correction is denoted using asterisks (*$P < 0.05$; **$P < 0.01$; ***$P < 0.001$)

	HINDBRAIN						MIDBRAIN		
	Olive			Vermis			Substantia nigra		
	Middle-aged	Elderly	Sig	Middle-aged	Elderly	Sig	Middle-aged	Elderly	Sig
14:0	1.84 ± 0.19	1.29 ± 0.12*	0.546	1.08 ± 0.05	0.99 ± 0.05	0.803	0.61 ± 0.02	0.65 ± 0.02	0.578
16:0	15.36 ± 0.26	15.78 ± 0.44	0.775	24.5 ± 0.56	24.7 ± 0.38	0.908	17.55 ± 0.18	18.28 ± 0.49	0.457
16:1n7	2.23 ± 0.09	2.11 ± 0.25	0.775	1.22 ± 0.08	1.14 ± 0.07	0.803	1.22 ± 0.03	1.35 ± 0.05*	0.229
18:0	20.11 ± 0.52	19.24 ± 0.81	0.597	20.28 ± 0.18	20.82 ± 0.48	0.803	22.57 ± 0.13	22.98 ± 0.29	0.571
18:1n9	30.57 ± 0.35	31.3 ± 2.48	0.597	20.81 ± 0.56	20.44 ± 0.84	0.813	24.1 ± 0.33	24.06 ± 1.00	0.947
18:1n7	5.19 ± 0.16	5.28 ± 0.17	0.917	4.37 ± 0.16	4.15 ± 0.13	0.803	5.08 ± 0.09	5.18 ± 0.19	0.805
18:2n6	0.62 ± 0.11	0.54 ± 0.09	0.775	0.94 ± 0.11	0.92 ± 0.07	0.944	0.73 ± 0.07	0.71 ± 0.061	0.879
18:3n3	0.18 ± 0.00	0.17 ± 0.01	0.775	0.07 ± 0.00	0.07 ± 0.00	0.803	0.11 ± 0.00	0.1 ± 0.00	0.571
18:4n3	0.05 ± 0.00	0.03 ± 0.00	0.597	0.03 ± 0.00	0.03 ± 0.00	0.803	0.02 ± 0.00	0.04 ± 0.00*	0.173
20:0	0.44 ± 0.09	0.38 ± 0.03	0.775	0.23 ± 0.00	0.28 ± 0.01**	0.068	0.24 ± 0.01	0.24 ± 0.00	0.947
20:1n9	4.54 ± 0.21	4.17 ± 0.68	0.775	1.40 ± 0.11	1.41 ± 0.14	0.946	2.31 ± 0.23	2.04 ± 0.15	0.578
20:2n6	0.86 ± 0.08	0.95 ± 0.12	0.774	0.29 ± 0.03	0.26 ± 0.01	0.803	0.45 ± 0.03	0.41 ± 0.04	0.658
20:3n6	1.53 ± 0.10	1.38 ± 0.11	0.753	1.02 ± 0.07	0.9 ± 0.06	0.803	1.42 ± 0.06	1.28 ± 0.12	0.571
20:4n6	4.3 ± 0.14	4.77 ± 0.73	0.565	8.02 ± 0.15	7.82 ± 0.28	0.803	6.95 ± 0.22	7.2 ± 0.23	0.607
20:5n3	0.05 ± 0.00	0.05 ± 0.01	0.981	0.05 ± 0.01	0.03 ± 0.01	0.803	0.14 ± 0.01	0.12 ± 0.01	0.571
22:0	0.4 ± 0.12	0.31 ± 0.04	0.775	0.07 ± 0.00	0.07 ± 0.00	0.944	0.13 ± 0.01	0.11 ± 0.01	0.578
22:1n9	0.83 ± 0.10	0.73 ± 0.79	0.775	0.85 ± 0.05	0.93 ± 0.06	0.803	0.96 ± 0.16	0.8 ± 0.34	0.616
22:4n6	3.78 ± 0.17	4.00 ± 0.22	0.774	2.96 ± 0.10	2.79 ± 0.26	0.803	4.67 ± 0.08	4.55 ± 0.18	0.689
22:5n6	0.24 ± 0.02	0.22 ± 0.13	0.775	0.75 ± 0.09	0.67 ± 0.12	0.813	0.46 ± 0.02	0.38 ± 0.12	0.457
22:5n3	0.20 ± 0.01	0.27 ± 0.02*	0.546	0.3 ± 0.019	0.27 ± 0.02	0.803	0.46 ± 0.02	0.45 ± 0.03	0.814
22:6n3	1.75 ± 0.20	2 .00 ± 1.14	0.774	9.92 ± 0.33	10.55 ± 0.32	0.803	7.58 ± 0.32	7.03 ± 0.46	0.571
24:0	1.12 ± 0.11	1.04 ± 0.17	0.775	0.11 ± 0.01	0.1 ± 0.01	0.803	0.05 ± 0.01	0.19 ± 0.03**	0.049
24:1n9	3.25 ± 0.14	3.27 ± 0.45	0.996	0.51 ± 0.08	0.5 ± 0.07	0.946	1.68 ± 0.19	1.4 ± 0.20	0.571
24:5n3	0.09 ± 0.00	0.11 ± 0.02	0.597	0.06 ± 0.00	0.05 ± 0.00	0.803	0.10 ± 0.01	0.12 ± 0.01	0.457
24:6n3	0.49 ± 0.03	0.61 ± 0.07*	0.546	0.16 ± 0.02	0.13 ± 0.01	0.803	0.41 ± 0.019	0.36 ± 0.04	0.501
ACL	18.39 ± 0.02	18.43 ± 0.06	0.775	18.31 ± 0.02	18.32 ± 0.03	0.9	18.53 ± 0.00	18.46 ± 0.01**	0.049
SFA	39.27 ± 0.35	38.03 ± 0.91	0.546	46.27 ± 0.66	46.95 ± 0.42	0.803	41.15 ± 0.24	42.45 ± 0.60*	0.228
UFA	60.73 ± 0.35	61.97 ± 0.91	0.546	53.73 ± 0.66	53.05 ± 0.42	0.803	58.85 ± 0.24	57.55 ± 0.60*	0.228
MUFA	46.61 ± 0.48	46.86 ± 2.88	0.874	29.16 ± 0.89	28.57 ± 1.17	0.813	35.36 ± 0.65	34.82 ± 1.06	0.738
PUFA	14.12 ± 0.46	15.11 ± 2.03	0.597	24.57 ± 0.44	24.48 ± 0.90	0.944	23.49 ± 0.48	22.73 ± 0.60	0.571
PUFAn3	2.79 ± 0.21	3.24 ± 1.05	0.597	10.59 ± 0.33	11.12 ± 0.34	0.803	8.81 ± 0.33	8.2 ± 0.44	0.571
PUFAn6	11.33 ± 0.26	11.87 ± 0.98	0.597	13.98 ± 0.26	13.36 ± 0.61	0.803	14.68 ± 0.31	14.53 ± 0.39	0.805
DBI	103.48 ± 2.01	108.63 ± 7.70	0.574	145.19 ± 1.90	145.55 ± 3.17	0.944	142.57 ± 1.87	137.95 ± 2.42	0.457
PI	59.9 ± 2.74	65.76 ± 12.88	0.597	135.75 ± 3.00	137.92 ± 4.95	0.813	122.52 ± 3.02	117.35 ± 4.36	0.571
SFA/UFA	0.65 ± 0.00	0.61 ± 0.02	0.546	0.86 ± 0.02	0.89 ± 0.01	0.803	0.7 ± 0.00	0.74 ± 0.01*	0.228

Table 2 (continued)

PβOx	3.69 ± 0.52		3.29 ± 7.47	0.775	74.66 ± 13.07	92.57 ± 14.00		0.803	19.17 ± 1.47	20.76 ± 6.38		0.716
	FOREBRAIN											
	DIENCEPHALON			SUBCORTICAL TELENCEPHALON								
	Thalamus			Hippocampus			Caudate			Putamen		
	Middle-aged	Elderly	Sig	Middle-aged	Elderly	Sig	Middle-aged	Elderly	Sig	Middle-aged	Elderly	Sig
14:0	0.67 ± 0.04	0.68 ± 0.04	0.976	0.88 ± 0.01	0.79 ± 0.18	0.759	0.63 ± 0.02	0.6 ± 0.07	0.671	0.62 ± 0.01	0.64 ± 0.05	0.809
16:0	18.08 ± 0.64	18.78 ± 0.91	0.934	20.99 ± 0.65	21.7 ± 0.65	0.759	21.46 ± 0.35	21.55 ± 0.50	0.932	19.39 ± 0.35	20.13 ± 0.57	0.568
16:1n7	1.34 ± 0.06	1.23 ± 0.14	0.761	1.26 ± 0.05	1.21 ± 0.22	0.759	0.92 ± 0.04	0.87 ± 0.05	0.673	0.89 ± 0.03	1.13 ± 0.11	0.309
18:0	23.36 ± 0.25	22.37 ± 0.59	0.687	22.01 ± 0.23	22.3 ± 0.39	0.759	25.41 ± 0.20	25.63 ± 0.98	0.693	24.05 ± 0.33	23.42 ± 0.37	0.470
18:1n9	23.06 ± 0.93	23.41 ± 1.55	0.937	20.88 ± 0.89	20.18 ± 1.21	0.759	17.43 ± 0.50	17.04 ± 0.64	0.762	18.49 ± 0.37	19.77 ± 0.98	0.470
18:1n7	4.51 ± 0.09	4.42 ± 0.30	0.934	4.69 ± 0.14	4.56 ± 0.28	0.759	4.69 ± 0.08	4.56 ± 0.11	0.682	4.48 ± 0.17	4.75 ± 0.12	0.520
18:2n6	0.66 ± 0.07	1.33 ± 0.59	0.687	0.64 ± 0.06	0.69 ± 0.05	0.759	1.03 ± 0.11	1.01 ± 0.10	0.942	1.08 ± 0.09	0.94 ± 0.21	0.632
18:3n3	0.09 ± 0.00	0.08 ± 0.00	0.761	0.06 ± 0.00	0.05 ± 0.01	0.759	0.07 ± 0.00	0.05 ± 0.00*	0.195	0.07 ± 0.00	0.07 ± 0.01	0.899
18:4n3	0.03 ± 0.00	0.04 ± 0.00	0.687	0.02 ± 0.00	0.02 ± 0.00	0.759	0.05 ± 0.00	0.04 ± 0.00	0.297	0.02 ± 0.00	0.02 ± 0.00	0.892
20:0	0.2 ± 0.00	0.33 ± 0.11	0.687	0.15 ± 0.01	0.15 ± 0.02	0.862	0.17 ± 0.00	0.2 ± 0.00*	0.195	0.17 ± 0.00	0.19 ± 0.01	0.394
20:1n9	1.74 ± 0.14	1.53 ± 0.25	0.796	1 ± 0.15	0.81 ± 0.39	0.759	0.85 ± 0.07	0.66 ± 0.10	0.297	1.03 ± 0.06	1.01 ± 0.14	0.934
20:2n6	0.36 ± 0.03	0.33 ± 0.04	0.687	0.45 ± 0.07	0.37 ± 0.08	0.759	0.17 ± 0.01	0.14 ± 0.02	0.368	0.22 ± 0.01	0.2 ± 0.02	0.763
20:3n6	0.9 ± 0.05	0.86 ± 0.08	0.796	1.25 ± 0.08	1.19 ± 0.07	0.759	1.03 ± 0.05	1.04 ± 0.07	0.935	1.03 ± 0.06	0.89 ± 0.06	0.394
20:4n6	7.76 ± 0.29	8.9 ± 1.03	0.687	8.82 ± 0.40	9.3 ± 0.70	0.759	9.23 ± 0.28	10.44 ± 0.42*	0.195	9.33 ± 0.21	9.45 ± 0.34	0.899
20:5n3	0.11 ± 0.01	0.11 ± 0.02	0.934	0.04 ± 0.01	0.04 ± 0.00	0.817	0.07 ± 0.00	0.08 ± 0.01	0.912	0.07 ± 0.01	0.06 ± 0.03	0.899
22:0	0.11 ± 0.01	0.18 ± 0.08	0.687	0.1 ± 0.01	0.09 ± 0.02	0.759	0.08 ± 0.00	0.07 ± 0.00	0.389	0.1 ± 0.00	0.09 ± 0.02	0.711
22:1n9	0.94 ± 0.03	0.81 ± 0.16	0.937	0.84 ± 0.10	0.55 ± 0.10*	0.705	1.32 ± 0.07	1.24 ± 0.12	0.671	1.02 ± 0.03	0.4 ± 0.25	0.579
22:4n6	5.12 ± 0.13	4.27 ± 0.26*	0.401	5.34 ± 0.09	4.96 ± 0.26*	0.705	4.72 ± 0.06	4.51 ± 0.11	0.297	5.38 ± 0.10	4.68 ± 0.27**	0.118
22:5n6	0.84 ± 0.08	0.6 ± 0.13	0.586	1.15 ± 0.11	1.03 ± 0.11	0.759	0.81 ± 0.06	0.63 ± 0.07	0.265	0.81 ± 0.05	0.56 ± 0.07*	0.202
22:5n3	0.34 ± 0.01	0.41 ± 0.04	0.586	0.3 ± 0.01	0.31 ± 0.02	0.759	0.28 ± 0.01	0.29 ± 0.02	0.673	0.31 ± 0.01	0.31 ± 0.01	0.987
22:6n3	7.69 ± 0.60	7.72 ± 0.96	0.937	7.64 ± 0.50	8.53 ± 0.93	0.759	8.52 ± 0.26	8.67 ± 0.34	0.839	10 ± 0.24	9.87 ± 0.57	0.899
24:0	0.34 ± 0.08	0.27 ± 0.05	0.796	0.03 ± 0.00	0.03 ± 0.09	0.759	0.17 ± 0.02	0.09 ± 0.01*	0.195	0.02 ± 0.00	0.02 ± 0.03*	0.309
24:1n9	1.39 ± 0.24	1.04 ± 0.23	0.694	1.14 ± 0.20	0.89 ± 0.20	0.759	0.69 ± 0.08	0.45 ± 0.08	0.27	1.14 ± 0.10	1.06 ± 0.20	0.899
24:5n3	0.05 ± 0.00	0.07 ± 0.00*	0.511	0.04 ± 0.00	0.04 ± 0.00	0.890	0.06 ± 0.00	0.06 ± 0.00	0.666	0.04 ± 0.00	0.06 ± 0.00	0.311
24:6n3	0.32 ± 0.04	0.25 ± 0.03	0.687	0.26 ± 0.04	0.2 ± 0.02	0.759	0.14 ± 0.01	0.09 ± 0.01*	0.195	0.26 ± 0.03	0.28 ± 0.05	0.899
ACL	18.53 ± 0.01	18.47 ± 0.01*	0.416	18.46 ± 0.01	18.44 ± 0.03	0.759	18.45 ± 0.00	18.44 ± 0.01	0.601	18.6 ± 0.01	18.51 ± 0.02**	0.167
SFA	42.75 ± 0.62	42.6 ± 1.26	0.937	44.17 ± 0.69	45.06 ± 0.71	0.759	47.91 ± 0.33	48.13 ± 0.50	0.839	44.35 ± 0.31	44.49 ± 0.91	0.913
UFA	57.25 ± 0.62	57.4 ± 1.26	0.937	55.83 ± 0.69	54.94 ± 0.71	0.759	52.09 ± 0.33	51.87 ± 0.50	0.839	55.65 ± 0.31	55.51 ± 0.91	0.913
MUFA	32.98 ± 1.34	32.44 ± 2.05	0.937	29.82 ± 1.30	28.21 ± 2.38	0.759	25.91 ± 0.71	24.82 ± 0.78	0.601	27.04 ± 0.55	28.12 ± 1.32	0.711
PUFA	24.27 ± 0.75	24.96 ± 1.06	0.796	26.01 ± 0.66	26.73 ± 1.82	0.759	26.18 ± 0.48	27.05 ± 0.47	0.535	28.61 ± 0.29	27.39 ± 0.63	0.319
PUFAn3	8.64 ± 0.58	8.68 ± 0.90	0.937	8.36 ± 0.47	9.19 ± 0.90	0.759	9.2 ± 0.24	9.28 ± 0.35	0.912	10.77 ± 0.20	10.66 ± 0.50	0.899
PUFAn6	15.64 ± 0.28	16.28 ± 1.30	0.796	17.65 ± 0.35	17.54 ± 0.94	0.863	16.98 ± 0.30	17.78 ± 0.41	0.379	17.84 ± 0.30	16.73 ± 0.29**	0.167
DBI	144.4 ± 2.97	145.16 ± 3.27	0.956	147.71 ± 2.51	150.64 ± 7.02	0.759	145.67 ± 1.56	148.21 ± 1.78	0.601	159.55 ± 0.88	155.72 ± 2.94	0.319
PI	127.6 ± 5.46	128.06 ± 6.90	0.976	133.56 ± 4.69	139.7 ± 11.29	0.759	136.66 ± 2.59	140.35 ± 2.68	0.625	152.54 ± 1.55	147.47 ± 4.76	0.470

Table 2 (continued)

SFA/UFA		0.75 ± 0.01	0.74 ± 0.04	0.937		0.79 ± 0.02	0.82 ± 0.02	0.759	0.92 ± 0.01	0.93 ± 0.01	0.839	0.8 ± 0.01	0.8 ± 0.03	0.899
PβOx		29.85 ± 3.86	33.91 ± 6.53	0.934		37.07 ± 6.16	48.54 ± 9.09	0.759	70.59 ± 11.74	109.16 ± 14.86	0.249	43.02 ± 5.80	48.88 ± 10.68	0.892
	FOREBRAIN													
	CORTICAL TELENCEPHALON													
	Occipital cortex					Parietal cortex			Temporal cortex					
	Middle-aged			Elderly	Sig	Middle-aged	Elderly	Sig	Middle-aged				Elderly	Sig
14:0	0.81 ± 0.03			0.7 ± 0.04	0.494	0.84 ± 0.04	0.7 ± 0.02*	0.557	0.82 ± 0.01				0.85 ± 0.03	0.773
16:0	21.76 ± 0.36			21.18 ± 0.37	0.825	21.11 ± 0.57	20.56 ± 0.49	0.846	24.73 ± 0.36				24.11 ± 0.83	0.503
16:1n7	1.17 ± 0.06			1.02 ± 0.13	0.705	1.3 ± 0.07	1.14 ± 0.07	0.846	0.98 ± 0.05				0.94 ± 0.10	0.773
18:0	24.52 ± 0.26			23.74 ± 0.49	0.494	24.38 ± 0.39	24.28 ± 0.38	0.973	24.87 ± 0.18				25.09 ± 0.12	0.756
18:1n9	17.89 ± 0.58			18.54 ± 0.92	0.977	19.72 ± 0.81	19.85 ± 0.63	0.973	15.11 ± 0.42				16.28 ± 0.69	0.231
18:1n7	3.94 ± 0.11			4.00 ± 0.19	0.982	4.3 ± 0.10	4.3 ± 0.26	0.996	3.33 ± 0.06				3.51 ± 0.19	0.699
18:2n6	1.05 ± 0.12			1.15 ± 0.12	0.977	1.21 ± 0.11	1.21 ± 0.13	0.996	0.94 ± 0.10				1.05 ± 0.10	0.773
18:3n3	0.06 ± 0.00			0.06 ± 0.00	0.982	0.08 ± 0.00	0.07 ± 0.00	0.846	0.04 ± 0.00				0.04 ± 0.00	0.978
18:4n3	0.03 ± 0.00			0.04 ± 0.00	0.494	0.04 ± 0.00	0.04 ± 0.00	0.973	0.03 ± 0.00				0.03 ± 0.00	0.823
20:0	0.19 ± 0.00			0.21 ± 0.00	0.494	0.21 ± 0.00	0.2 ± 0.00	0.973	0.16 ± 0.00				0.18 ± 0.00*	0.147
20:1n9	1.03 ± 0.09			1.02 ± 0.11	0.987	1.19 ± 0.16	1.04 ± 0.16	0.863	0.46 ± 0.05				0.52 ± 0.17	0.773
20:2n6	0.25 ± 0.02			0.21 ± 0.02	0.817	0.30 ± 0.03	0.25 ± 0.01	0.846	0.16 ± 0.01				0.15 ± 0.05	0.773
20:3n6	0.99 ± 0.05			0.97 ± 0.07	0.982	1.08 ± 0.054	1.02 ± 0.07	0.863	1.11 ± 0.07				1.02 ± 0.06	0.756
20:4n6	7.33 ± 0.23			7.38 ± 0.31	0.982	7.71 ± 0.32	8.02 ± 0.27	0.876	9.96 ± 0.31				9.1 ± 0.41	0.231
20:5n3	0.06 ± 0.012			0.06 ± 0.00	0.982	0.07 ± 0.00	0.06 ± 0.02	0.921	0.08 ± 0.01				0.07 ± 0.00	0.773
22:0	0.09 ± 0.00			0.10 ± 0.00	0.982	0.11 ± 0.01	0.11 ± 0.01	0.973	0.05 ± 0.00				0.06 ± 0.01	0.756
22:1n9	2.18 ± 0.10			2.28 ± 0.27	0.982	0.74 ± 0.04	0.48 ± 0.07	0.846	0.86 ± 0.39				1.07 ± 0.20	0.782
22:4n6	3.9 ± 0.13			3.51 ± 0.12	0.494	4.08 ± 0.13	3.88 ± 0.12	0.846	4.43 ± 0.11				4.04 ± 0.15*	0.173
22:5n6	0.78 ± 0.05			0.65 ± 0.09	0.592	0.84 ± 0.09	0.72 ± 0.09	0.846	0.96 ± 0.08				0.66 ± 0.06*	0.164
22:5n3	0.33 ± 0.01			0.37 ± 0.02	0.502	0.3 ± 0.01	0.34 ± 0.03	0.759	0.34 ± 0.02				0.36 ± 0.03	0.773
22:6n3	10.49 ± 0.29			11.69 ± 0.59	0.502	8.95 ± 0.43	10.37 ± 0.46	0.557	10.04 ± 0.27				10.4 ± 0.57	0.756
24:0	0.14 ± 0.019			0.13 ± 0.032	0.982	0.22 ± 0.04	0.2 ± 0.03	0.973	0.04 ± 0.00				0.06 ± 0.04	0.509
24:1n9	0.80 ± 0.10			0.80 ± 0.16	0.987	0.97 ± 0.22	0.83 ± 0.13	0.936	0.24 ± 0.06				0.28 ± 0.22	0.773
24:5n3	0.04 ± 0.00			0.03 ± 0.00	0.792	0.05 ± 0.00	0.07 ± 0.01	0.742	0.06 ± 0.00				0.04 ± 0.00*	0.147
24:6n3	0.16 ± 0.01			0.17 ± 0.02	0.982	0.19 ± 0.02	0.26 ± 0.07	0.846	0.19 ± 0.02				0.09 ± 0.03**	0.057
ACL	18.49 ± 0.01			18.54 ± 0.01*	0.494	18.42 ± 0.02	18.47 ± 0.01	0.557	18.39 ± 0.01				18.38 ± 0.02	0.773
SFA	47.51 ± 0.47			46.05 ± 0.71	0.494	46.88 ± 0.76	46.05 ± 0.78	0.846	50.68 ± 0.46				50.35 ± 0.77	0.773
UFA	52.49 ± 0.47			53.95 ± 0.71	0.494	53.12 ± 0.76	53.95 ± 0.78	0.846	49.32 ± 0.46				49.65 ± 0.77	0.773

Table 2 (continued)

MUFA	27.02 ± 0.85		27.66 ± 1.38	0.982	28.22 ± 1.23	27.66 ± 1.17	0.973	20.98 ± 0.71	22.6 ± 1.53	0.254
PUFA	25.48 ± 0.48		26.3 ± 0.85	0.825	24.91 ± 0.54	26.3 ± 0.43	0.646	28.34 ± 0.46	27.06 ± 0.86	0.231
PUFAn3	11.17 ± 0.29		12.43 ± 0.58	0.494	9.68 ± 0.41	11.19 ± 0.42*	0.557	10.77 ± 0.31	11.03 ± 0.57	0.773
PUFAn6	14.3 ± 0.39		13.86 ± 0.30	0.793	15.22 ± 0.36	15.11 ± 0.30	0.973	17.57 ± 0.42	16.02 ± 0.33*	0.147
DBI	147.77 ± 1.58		153.92 ± 3.38	0.500	143.21 ± 1.98	151.26 ± 1.78*	0.557	152.85 ± 1.72	149.47 ± 3.06	0.517
PI	141.57 ± 2.60		149.4 ± 5.77	0.705	132.58 ± 3.79	144.17 ± 3.66	0.557	152.02 ± 2.57	147.29 ± 5.51	0.517
SFA/UFA	0.91 ± 0.01		0.85 ± 0.024	0.494	0.89 ± 0.02	0.85 ± 0.02	0.846	1.03 ± 0.01	1.01 ± 0.02	0.773
PβOx	84.36 ± 14.11		80.57 ± 17.42	0.982	58.46 ± 12.84	60.12 ± 13.10	0.973	61.01 ± 11.706	135.92 ± 22.40**	0.057
		FOREBRAIN								
		CORTICAL TELENCEPHALON								
		Entorhinal cortex			Frontal cortex			Cingulate cortex		
		Middle-aged	Elderly	Sig	Middle-aged	Elderly	Sig	Middle-aged	Elderly	Sig
14:0		0.79 ± 0.03	0.81 ± 0.03	0.866	0.84 ± 0.04	0.77 ± 0.04	0.953	0.95 ± 0.05	0.87 ± 0.03	0.934
16:0		20.98 ± 0.66	20.03 ± 0.85	0.695	22.16 ± 0.51	22.09 ± 0.36	0.964	23.73 ± 0.93	22.52 ± 0.80	0.934
16:1n7		1.29 ± 0.07	1.52 ± 0.17	0.691	1.38 ± 0.08	1.28 ± 0.08	0.953	1.38 ± 0.12	1.52 ± 0.15	0.934
18:0		24.38 ± 0.27	23.82 ± 0.36	0.691	24.33 ± 0.26	24.28 ± 0.49	0.964	22.79 ± 0.41	22.49 ± 0.42	0.934
18:1n9		18.74 ± 0.95	20.86 ± 1.28	0.691	17.94 ± 0.84	18.03 ± 0.56	0.964	18.56 ± 1.18	19.53 ± 0.87	0.934
18:1n7		4.05 ± 0.16	4.11 ± 0.22	0.908	3.91 ± 0.11	3.85 ± 0.25	0.964	3.97 ± 0.11	4.14 ± 0.28	0.934
18:2n6		0.78 ± 0.08	0.83 ± 0.09	0.866	1.13 ± 0.07	1.12 ± 0.10	0.964	0.81 ± 0.10	0.86 ± 0.08	0.934
18:3n3		0.05 ± 0.00	0.06 ± 0.00	0.695	0.06 ± 0.00	0.05 ± 0.00	0.953	0.06 ± 0.00	0.07 ± 0.00	0.934
18:4n3		0.03 ± 0.00	0.03 ± 0.00	0.759	0.04 ± 0.00	0.03 ± 0.00	0.953	0.03 ± 0.00	0.03 ± 0.00	0.934
20:0		0.21 ± 0.00	0.23 ± 0.01	0.691	0.25 ± 0.08	0.19 ± 0.01	0.953	0.19 ± 0.00	0.22 ± 0.00**	0.376
20:1n9		0.88 ± 0.15	1.06 ± 0.14	0.705	0.82 ± 0.10	0.76 ± 0.09	0.964	0.94 ± 0.23	1.07 ± 0.18	0.934
20:2n6		0.31 ± 0.04	0.32 ± 0.03	0.975	0.24 ± 0.02	0.21 ± 0.03	0.953	0.3 ± 0.04	0.28 ± 0.04	0.934
20:3n6		1.02 ± 0.07	0.97 ± 0.06	0.851	1.05 ± 0.04	0.99 ± 0.10	0.953	1 ± 0.05	0.98 ± 0.07	0.970
20:4n6		8.91 ± 0.37	8.17 ± 0.34	0.691	8.38 ± 0.30	8.56 ± 0.28	0.964	8.12 ± 0.30	7.75 ± 0.35	0.934
20:5n3		0.06 ± 0.00	0.06 ± 0.01	0.866	0.08 ± 0.01	0.05 ± 0.00	0.953	0.06 ± 0.01	0.05 ± 0.01	0.934
22:0		0.09 ± 0.01	0.12 ± 0.01	0.691	0.08 ± 0.00	0.08 ± 0.00	0.953	0.08 ± 0.01	0.09 ± 0.01	0.934
22:1n9		0.7 ± 0.04	0.62 ± 0.06	0.691	1.04 ± 0.12	0.96 ± 0.07	0.964	0.75 ± 0.07	0.72 ± 0.07	0.934
22:4n6		4.94 ± 0.10	4.75 ± 0.17	0.691	4.1 ± 0.11	3.91 ± 0.23	0.953	4.72 ± 0.14	4.48 ± 0.15	0.934
22:5n6		0.88 ± 0.05	0.68 ± 0.13	0.691	0.96 ± 0.10	0.73 ± 0.16	0.953	1.03 ± 0.12	0.78 ± 0.08	0.934
22:5n3		0.3 ± 0.01	0.31 ± 0.02	0.908	0.31 ± 0.01	0.34 ± 0.02	0.953	0.3 ± 0.02	0.32 ± 0.02	0.934
22:6n3		9.29 ± 0.44	8.72 ± 0.78	0.763	9.97 ± 0.49	10.87 ± 0.53	0.953	9.08 ± 0.62	9.84 ± 0.57	0.934
24:0		0.23 ± 0.053	0.34 ± 0.07	0.691	0.16 ± 0.03	0.14 ± 0.02	0.964	0.2 ± 0.08	0.22 ± 0.04	0.970

Table 2 (continued)

24:1n9	0.85 ± 0.19	1.32 ± 0.31	0.691	0.58 ± 0.17	0.54 ± 0.11	0.964	0.74 ± 0.29	0.93 ± 0.24	0.934	
24:5n3	0.04 ± 0.00	0.05 ± 0.00	0.695	0.05 ± 0.00	0.04 ± 0.00	0.953	0.04 ± 0.00	0.04 ± 0.00	0.934	
24:6n3	0.17 ± 0.03	0.23 ± 0.04	0.695	0.13 ± 0.02	0.12 ± 0.01	0.964	0.15 ± 0.04	0.18 ± 0.03	0.934	
ACL	18.48 ± 0.01	18.48 ± 0.01	0.975	18.43 ± 0.00	18.44 ± 0.01	0.953	18.38 ± 0.02	18.42 ± 0.01	0.934	
SFA	46.68 ± 0.82	45.36 ± 1.07	0.691	47.83 ± 0.60	47.56 ± 0.52	0.964	47.95 ± 1.10	46.41 ± 0.91	0.934	
UFA	53.32 ± 0.82	54.64 ± 1.07	0.691	52.17 ± 0.60	52.44 ± 0.52	0.964	52.05 ± 1.10	53.59 ± 0.91	0.934	
MUFA	26.52 ± 1.39	29.48 ± 2.00	0.691	25.68 ± 1.20	25.42 ± 0.86	0.964	26.34 ± 1.90	27.93 ± 1.58	0.934	
PUFA	26.8 ± 0.58	25.16 ± 0.95	0.691	26.49 ± 0.68	27.02 ± 0.41	0.953	25.71 ± 0.85	25.67 ± 0.69	0.970	
PUFAn3	9.95 ± 0.41	9.45 ± 0.73	0.787	10.63 ± 0.47	11.5 ± 0.53	0.953	9.73 ± 0.59	10.53 ± 0.56	0.934	
PUFAn6	16.85 ± 0.26	15.71 ± 0.33*	0.691	15.86 ± 0.32	15.52 ± 0.63	0.953	15.98 ± 0.34	15.13 ± 0.46	0.934	
DBI	150.66 ± 2.00	145.79 ± 3.38	0.691	149.4 ± 2.67	152.96 ± 1.19	0.953	145.79 ± 2.83	148.5 ± 2.14	0.934	
PI	142.85 ± 4.21	133.85 ± 6.83	0.691	143.49 ± 4.71	148.97 ± 2.63	0.953	137.84 ± 5.74	140.32 ± 4.55	0.934	
SFA/UFA	0.88 ± 0.02	0.83 ± 0.03	0.691	0.92 ± 0.02	0.91 ± 0.01	0.964	0.93 ± 0.03	0.87 ± 0.03	0.934	
PβOx	79.71 ± 15.08	58.42 ± 20.69	0.732	91.97 ± 13.39	105.31 ± 16.42	0.953	84.06 ± 12.88	75.12 ± 18.50	0.934	

elongase and desaturase activity was estimated from specific product/substrate ratios. The outcomes confirm the existence of minor changes induced by aging across the different brain regions (Supplementary Table S1). Overall, the higher estimated desaturase activity corresponds first to delta-5-desaturase (D5D, r20:4n-6/20:3n-6), and then to delta-6-desaturase (b) (D6D (b), r24:6n-3/24:5n-3), with D5D being systematically higher than D6D in all brain regions with the only exception of olive (medulla oblongata), where D6D is higher than D5D. For elongases, the higher activity corresponds to Elovl2-5 (n-3) (r22:5n-3/20:5n-3) followed by Elovl3 (n-9) (c) (r24:1n-9/22:1n-9) and Elovl6 (r18:0/16:0); this observation is maintained in all brain regions.

Brain regional changes in estimated desaturase and elongase activity: comparison of middle-aged and elderly groups

The changes observed on the elderly compared with the middle-aged group were region-dependent. Specifically, in the hindbrain, a reduced Elovl1-3–7 (a) ($p < 0.01$) and (b) ($p < 0.05$) estimated activity in *vermis* was observed. In the midbrain, *substantia nigra* showed an increased estimated D6D (a) ($p < 0.05$), Elovl1-3–7 (c) ($p < 0.001$), and Elovl2 activity ($p < 0.05$), and decrease in D6D (b) activity ($p < 0.05$). In the diencephalon, *thalamus* D6D (b) and Elovl2-5 (n-6) estimated activity was decreased ($p < 0.05$ and $p < 0.05$, respectively). In the subcortical telencephalon, a reduced estimated activity of Elovl1-3–7 (b) and (c) ($p < 0.01$ and $p < 0.05$, respectively), Elovl3 (a) ($p < 0.05$), and Elovl2-5(n-6) ($p < 0.05$), and very slight increase of Elovl1-3–7 (a) ($p < 0.05$) activity were found in the *caudate nucleus*, whereas in the *putamen nucleus* Elovl1-3–7 (b) activity was decreased ($p < 0.05$) along with an enhanced Elovl1-3–7 (c) and Elovl2 activity (both $p < 0.05$). Finally, in the six regions of the human cerebral cortex (cortical telencephalon), little changes were observed and included a very small increase in Elovl1-3–7 (a) activity ($p < 0.05$) in the *occipital cortex*, reduced D6D (b) ($p < 0.05$) and Elovl2 ($p < 0.05$) along with an enhanced Elovl6 ($p < 0.05$) and Elovl1-3–7 (a) ($p < 0.05$) estimated activity in the *temporal cortex*, and a slight increase of Elovl1-3–7 (a) ($p < 0.05$) in *cingulate cortex*. No changes in the estimated enzymatic activity were detected in *olive*

(hindbrain), *hippocampus* (*subcortical telencephalon*), and *parietal*, *entorhinal*, and *frontal cortex* (cortical telencephalon). These results suggest a global increase of the Elovl1-3–7 (a) along with a reduced Elovl1-3–7 (b) and D6D (b) estimated activities in the elderly.

Because of the large number of tests, adjustment for multiple comparisons was assessed using the Benjamini–Hochberg false discovery rate (FDR) analysis. *p* values when comparing the two groups of cases are shown in Table S1. As a result, only elovl3-7 (b) and (c) and elovl2 in putamen were sustained following multiple comparison adjustment.

Brain regional changes in lipid composition as a function of age

An additional approach was used to learn about the lipid composition changes as a function of age, as a continuous variable instead of dichotomizing the data into a middle-aged and an elderly cohort. To this end, the existence of correlations between fatty acid composition and age was evaluated by applying a Spearman correlation test. Results are presented in Supplementary Table S2 and Figs. 1, 2, 3, 4, 5, 6, and 7. Remarkably, in addition to previously observed changes in fatty acid composition with age comparing middle-aged vs elderly groups (also confirmed by the correlation analysis), new relationships appeared as a continuum with the correlation analysis in diverse brain regions. Reinforcing our findings, potential interference of the variables of gender and post-mortem time (PMT) in the age-based trajectories of the different fatty acids and indexes was ruled out after applying the corresponding statistical analysis (data not shown).

More specifically, in the hindbrain, the correlation analysis did not provide additional changes with age in *olive* and *vermis* (Fig. 1). In the midbrain, in *substantia nigra*, an additional negative correlation was detected in PUFA ($p=0.025$) content and DBI ($p=0.023$) with age (Fig. 1). In the diencephalon, in *thalamus*, an increase in the content of 22:5n-3 ($p=0.023$) was added (Fig. 2). In the subcortical telencephalon, in the *hippocampus*, an increase in PUFAn-3 ($p=0.034$), and in the *putamen*, an increase with age in the content of 16: 0 ($p=0.022$) and 24:5n-3 ($p=0.006$) was additionally observed (Fig. 2). Especially noteworthy is the amplitude of the additional change detected in the *caudate*, with a decrease in the content of the fatty acids 20:1n-9 ($p=0.03$), 22:4n-6 ($p=0.007$), 22:5n-6 ($p=0.049$), and 24:1n-9 ($p=0.033$) (Fig. 2). At the cortical telencephalon level, the following new correlations should be highlighted: in *occipital cortex*, decrease in content of 18:0 ($p=0.012$); in *parietal cortex*, decrease in content of 14:0 ($p=0.027$), and increase in content of 22:6n-3 ($p=0.007$) and, concomitantly, ACL ($p=0.006$), PUFA ($p=0.015$), and PI ($p=0.019$); in *entorhinal cortex*, the increase in 20:0 ($p=0.017$); and in *frontal cortex*, the increase in 20:0 ($p=0.023$), and the decrease in 22:5n-6 ($p=0.018$) (Fig. 3). *Cingulate cortex* and *temporal cortex* require special mention.

Cingulate cortex, which is located in the medial region of the cortical telencephalon, appears to be the region most affected by the aging process out of the thirteen included in the present study (Tables 2, S1 and S2, and Fig. 4). Thus, in addition to the increased content of 20:0 ($p<0.01$) detected in the comparison between middle-age vs elderly individuals, the following new correlations should be added: decreased content with age of 16:0 ($p=0.008$), 20:4n-6 ($p=0.025$), 22:5n-6 ($p=0.018$), SFA ($p=0.008$), PUFAn-6 ($p=0.003$), and ratio SFA/UFA ($p=0.008$); and increased content with age of 16:1n-7 ($p=0.024$), 18:1n-9 ($p=0.026$), 20:1n-9 ($p=0.04$), 22:0 ($p=0.023$), 24:0 ($p=0.021$), 24:1n-9 ($p=0.018$), 24:6n-3 ($p=0.019$), ACL ($p=0.009$), UFA ($p=0.008$), and MUFA ($p=0.027$). Globally, these changes may be attributed to enhanced metabolic activity of the elongases and desaturases involved in the biosynthesis of SFA and MUFA from 16:0 (Table S2 and Fig. 5A).

Fatty acid composition of an additional region located in the cortical telencephalon, the *inferior temporal cortex*, is also profoundly affected by the aging process (Tables 2, S1 and S2, and Fig. 6). Thus, aside from the changes detected in the comparison between middle-age and elderly individuals, the correlation analysis did provide additional changes with age. Thus, a decrease in the content of 20:4n-6 ($p=0.034$), 22:4n-6 ($p=0.002$), 22:5n-6 ($p=0.006$), 24:5n-3 ($p=0.024$), 24:6n-3 ($p=0.011$), ACL ($p=0.04$), PUFA ($p=0.022$), PUFAn-6 ($p=0.001$), DBI ($p=0.033$), and PI ($p=0.047$) was observed with age; while 18:1n-9 ($p=0.001$), MUFA ($p=0.02$), and

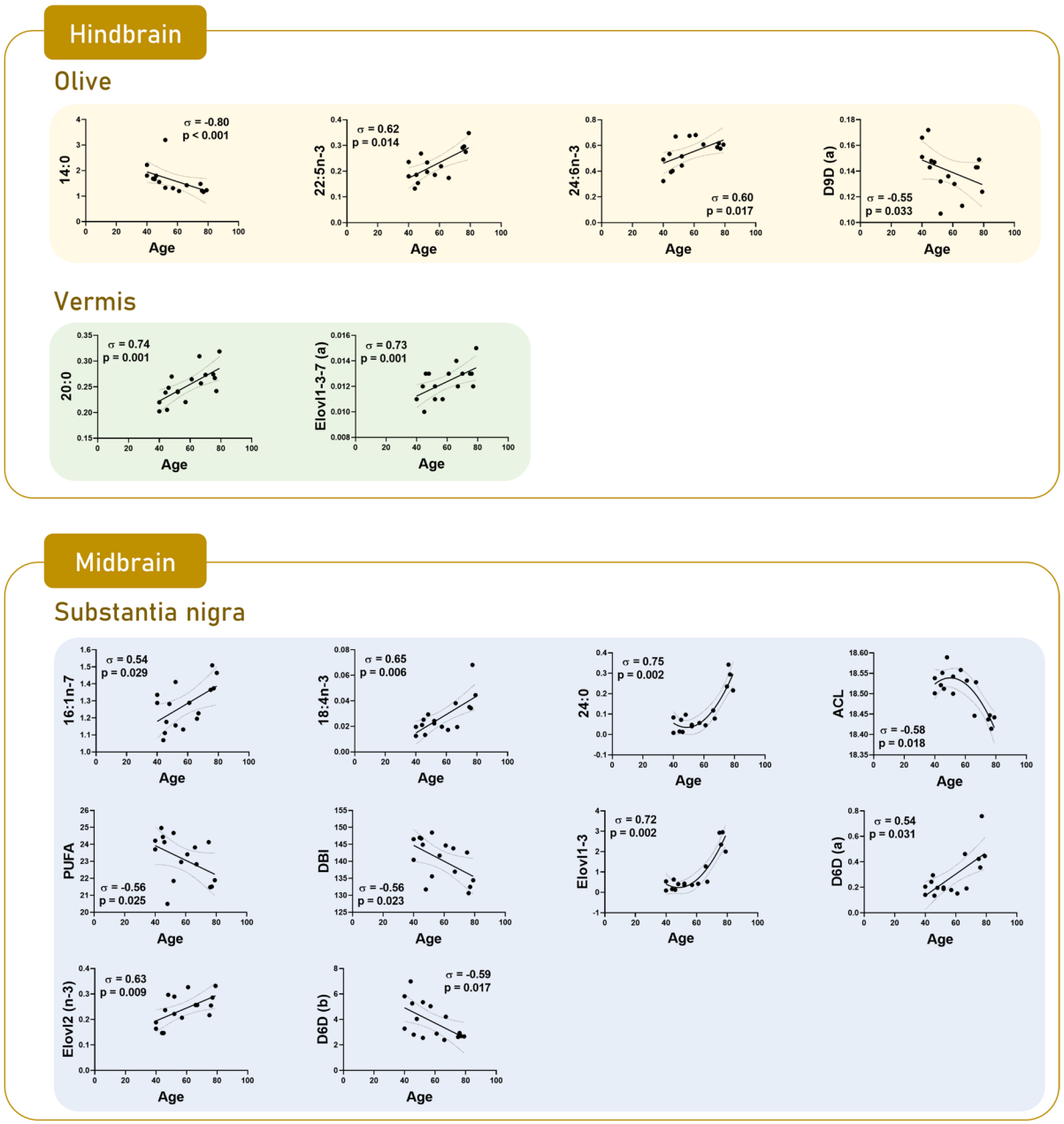

Fig. 1 Scatterplots by region based on significant correlations between fatty acids and calculated indexes and age in hindbrain and midbrain: olive, vermis, and substantia nigra

peroxisomal β-oxidation activity ($p=0.001$) showed an increase with age. All these changes are suggestive of alterations with age in the PUFAn-6 biosynthesis pathway, as well as at the peroxisomal level (Fig. 5B).

Adjustment for multiple correlations was assessed using the Benjamini–Hochberg false discovery rate (FDR) analysis. p values at FDR 10% are shown in Table 3 and Table S2. After correction, fatty acid content and derived indexes in *substantia nigra*, *hippocampus*, *caudate*, *occipital cortex*, *parietal cortex*, *entorhinal cortex*, *frontal cortex*, and age as a continuum were no longer significant. Significant

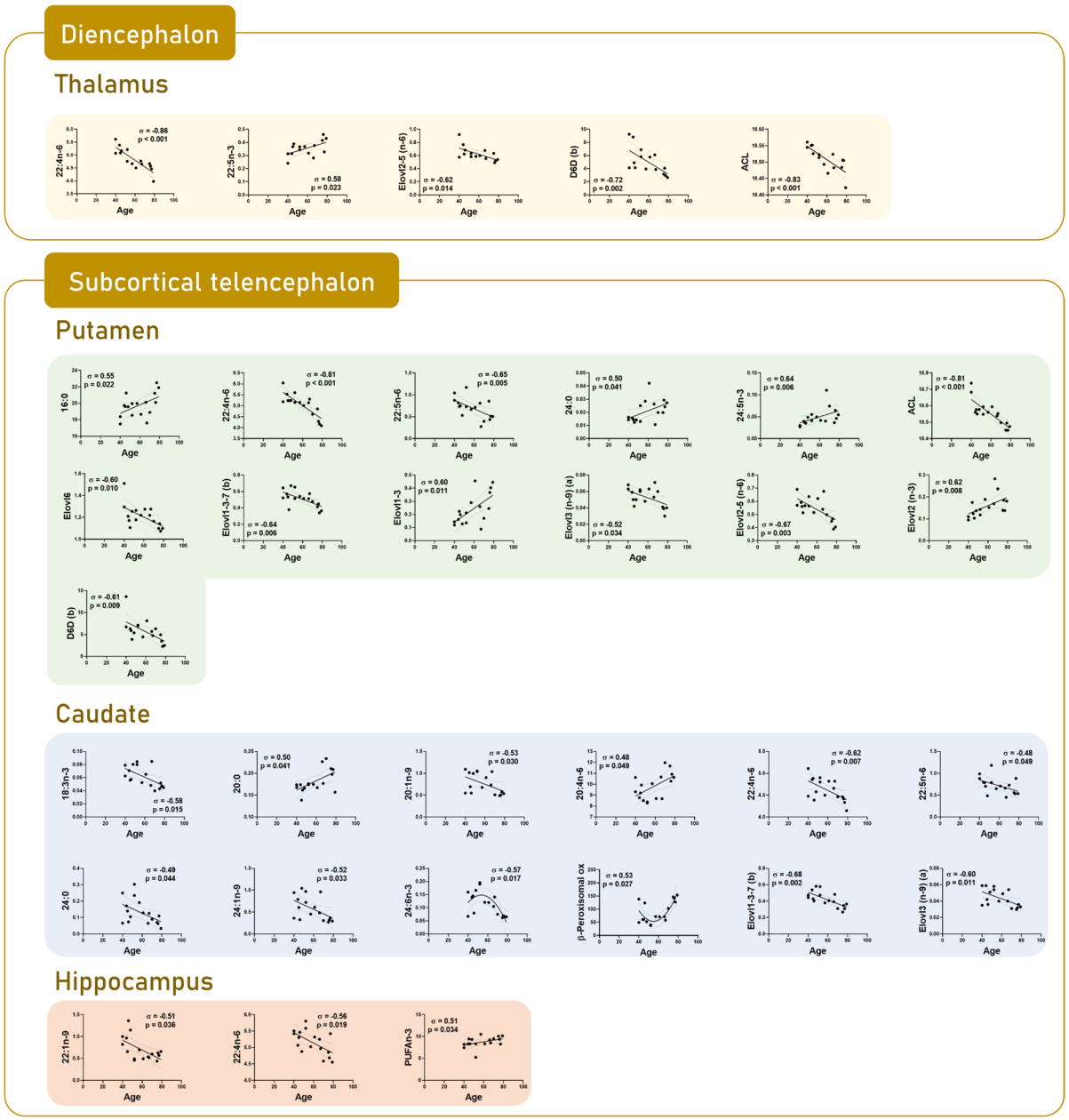

Fig. 2 Scatterplots by region based on significant correlations between fatty acids and calculated indexes and age in diencephalon and subcortical telencephalon: thalamus, anterior putamen, head of the caudate, and hippocampus

correlations were maintained in *olive* for 14:0 ($p=0.001$); in *vermis* for 20:0 ($p=0.035$); in *thalamus* for 22:4n-6 ($p=0.001$) and ACL ($p=0.001$); in *putamen* for 22:4n-6 ($p=0.001$) and ACL ($p=0.001$); in *temporal inferior cortex* for 18:1n-9 ($p=0.018$), 22:4n-6 ($p=0.023$) and PUFAn-6 ($p=0.018$), and in *cingulate cortex* for 16:0 ($p=0.045$), 20:0 ($p=0.045$), ACL ($p=0.045$), SFA ($p=0.045$), UFA ($p=0.045$), PUFAn-6 ($p=0.045$), and ratio SFA/UFA ($p=0.045$).

Finally, we have developed a series of correlation matrixes for integrative indexes in order to evaluate the existence of regional relationships (Fig. 7). The results show that the regional relationships are very restricted without apparent general patterns.

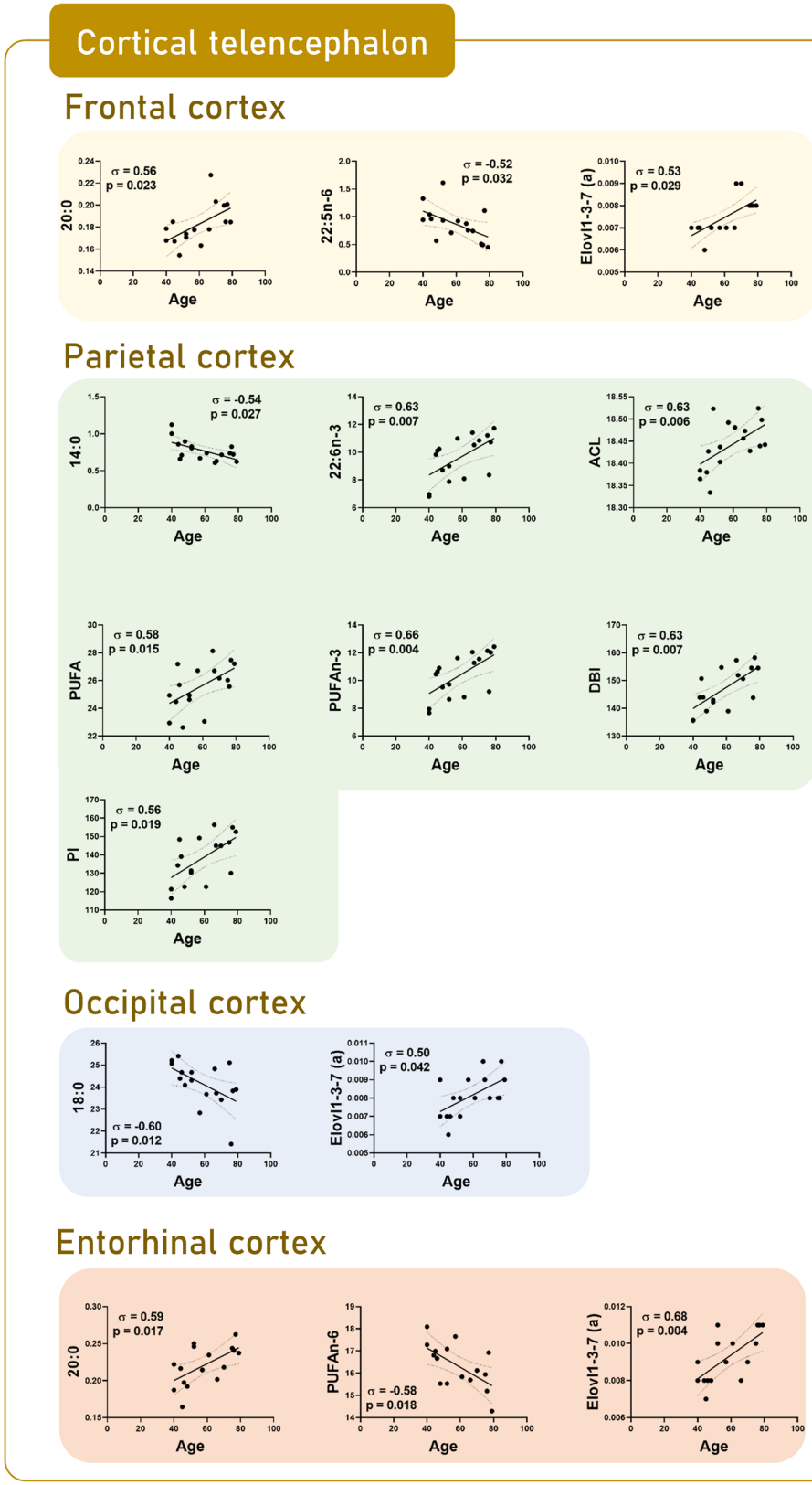
Cortical telencephalon
Frontal cortex
20:0
σ = 0.56
p = 0.023
22:5n-6
σ = -0.52
p = 0.032
Elovl1-3-7 (a)
σ = 0.53
p = 0.029
Parietal cortex
14:0
σ = -0.54
p = 0.027
22:6n-3
σ = 0.63
p = 0.007
ACL
σ = 0.63
p = 0.006
PUFA
σ = 0.58
p = 0.015
PUFAn-3
σ = 0.66
p = 0.004
DBI
σ = 0.63
p = 0.007
PI
σ = 0.56
p = 0.019
Occipital cortex
18:0
σ = -0.60
p = 0.012
Elovl1-3-7 (a)
σ = 0.50
p = 0.042
Entorhinal cortex
20:0
σ = 0.59
p = 0.017
PUFAn-6
σ = -0.58
p = 0.018
Elovl1-3-7 (a)
σ = 0.68
p = 0.004
Age

◂**Fig. 3** Scatterplots by region based on significant correlations between fatty acids and calculated indexes and age in cortical telencephalon: frontal cortex area 8, parietal cortex area 7, occipital cortex areas 17–18, and entorhinal cortex

The index with the greatest regional relationships is PUFAn-6.

Discussion

The human brain aging process induces changes at all levels of biological organization, although with a heterogeneous interregional impact, which demands adaptive responses in order to preserve the composition and function within physiological limits. The lipid bilayer that composes neuronal and glial cell membranes is not on the sidelines; consequently, the longer the optimal membrane lipid profile is sustained, the better neural cell function and survival.

The first evidence of changes in the lipid profile in the human brain during aging revealed, analyzing the whole brain, that there is a slow and progressive decrease with age in the total lipid content from the second-third decade of life [17–19]. Later on, different studies analyzing specific lipid classes (mostly glycerophospholipids) in diverse regions of human brain confirmed the occurrence of age-related lipid changes in terms of a decreased phospholipid content which is again very slow and progressive throughout the adult lifespan and varying in a region-dependent way [20, 21], but is accelerated at advanced age (over 80 years old) [21–24]. Furthermore, human brain cholesterol content also showed a very similar behavior

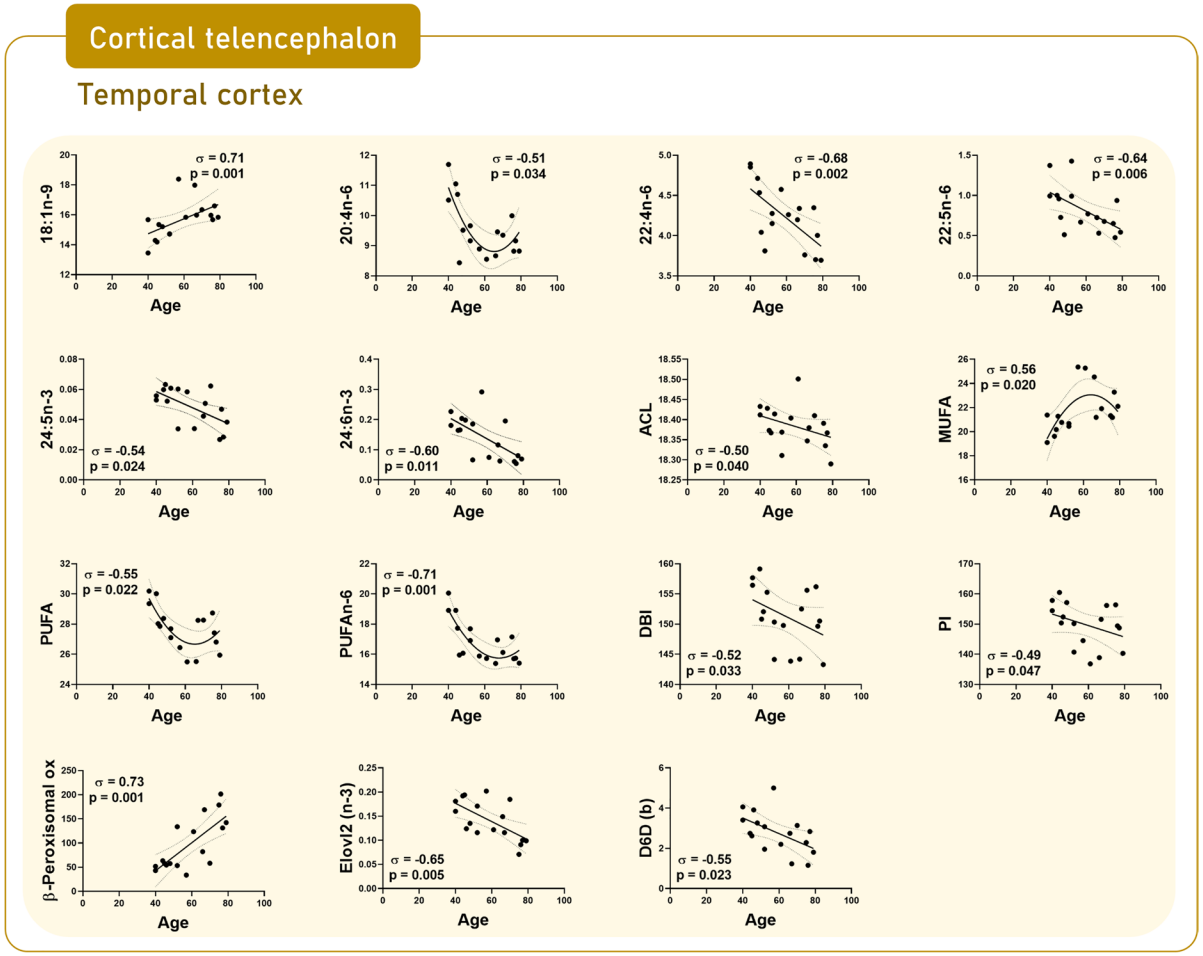

Fig. 4 Scatterplots by region based on significant correlations between fatty acids and calculated indexes and age in cingulate gyrus (area 24)

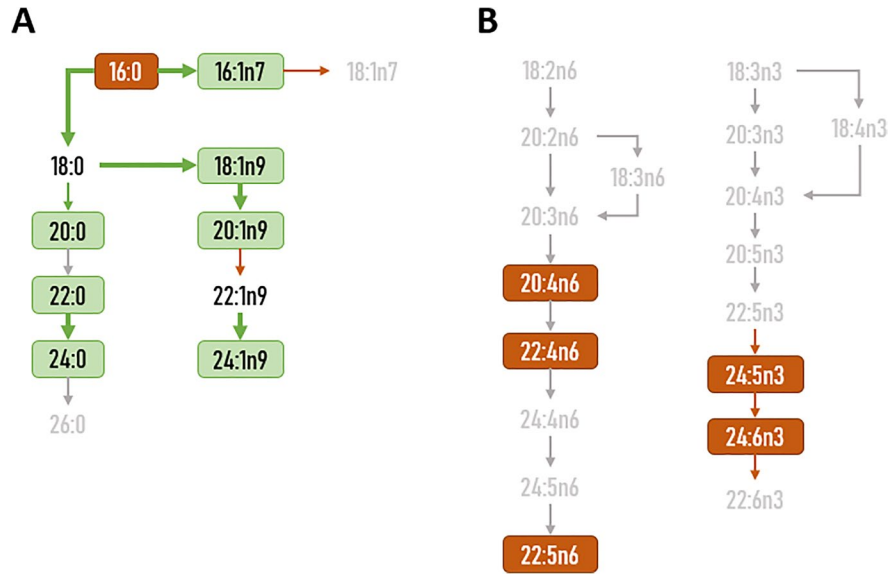

Fig. 5 Cingulate cortex (**A**) and temporal cortex (**B**) changes in fatty acid composition associated with the aging process. Figure is based on data presented in Tables 1 and 2 and Figs. 4 and 6. Green boxes and rows represent increased content of individual FA or enhanced estimated activity in aged individuals compared to the middle-aged. Orange boxes and rows represent reduced content of individual FA or decreased estimated activity in aged individuals compared to the middle-aged. Gray text and rows represent unchanged content of individual FA or estimated activity in aged individuals compared to the middle-aged

with age [21, 24]. More recent studies analyzing the microsomal and mitochondrial lipidome, particularly the main phospholipid classes, of entorhinal cortex, frontal cortex, and hippocampus of subjects from 20 to 100 years old, found that minor fractions of phospholipids specifically containing PUFAn-6 slightly decrease during adult life, while phospholipid species containing PUFAn-3 increase during the same period [25–27]. In this line of minor changes with age, and even compositional stability during adult life, no significant changes were observed in the different classes of lipids and composition in fatty acids of human frontal cortex membrane microdomains (lipid rafts) in subjects with an age range between 24 and 85 years [28].

The fatty acid profile and its changes with aging have also been the subject of study in various works. In these studies, different regions of the human cerebral cortex such as frontal cortex (area 8) [29, 30], prefrontal cortex [26], orbitofrontal cortex (area 10) [31], entorhinal cortex [27], and hippocampus [25] of healthy adults with an age ranging from 20 to 80 years were analyzed. Globally, the outcomes of these studies suggest a general preservation of the fatty acid composition during adult life with minor changes, if at all, preferentially expressed as a decrease in PUFAn-6 content, and maintenance or slight increase in PUFAn-3 content, with and eventual fall at more advanced ages. Our findings reinforce these previous observations in frontal cortex, entorhinal cortex, and hippocampus, and extend this relative preservation of the fatty acid profile to other human brain regions such as olive (medulla oblongata), upper vermis (cerebellum), substantia nigra, thalamus, head of the caudate nucleus, anterior putamen, occipital (visual) cortex, and parietal cortex. In contrast, cingulate gyrus and inferior temporal cortex showed an entirely different tendency, with broad involvement of their fatty acid profiles.

Inferior temporal cortex area 20 and cingulate gyrus area 24 are the two brain regions most affected by aging, showing the most extensive changes in fatty acid profiles. Notably, the two regions share some changes, while others are region specific, highlighting the increased content in MUFAs, ascribed to the 18:1n-9 acyl chain, and decreased content of PUFAn-6, basically due to a decreased content of 20:4n-6 and 22:5n-6. While the 18:1n-9 increase could be

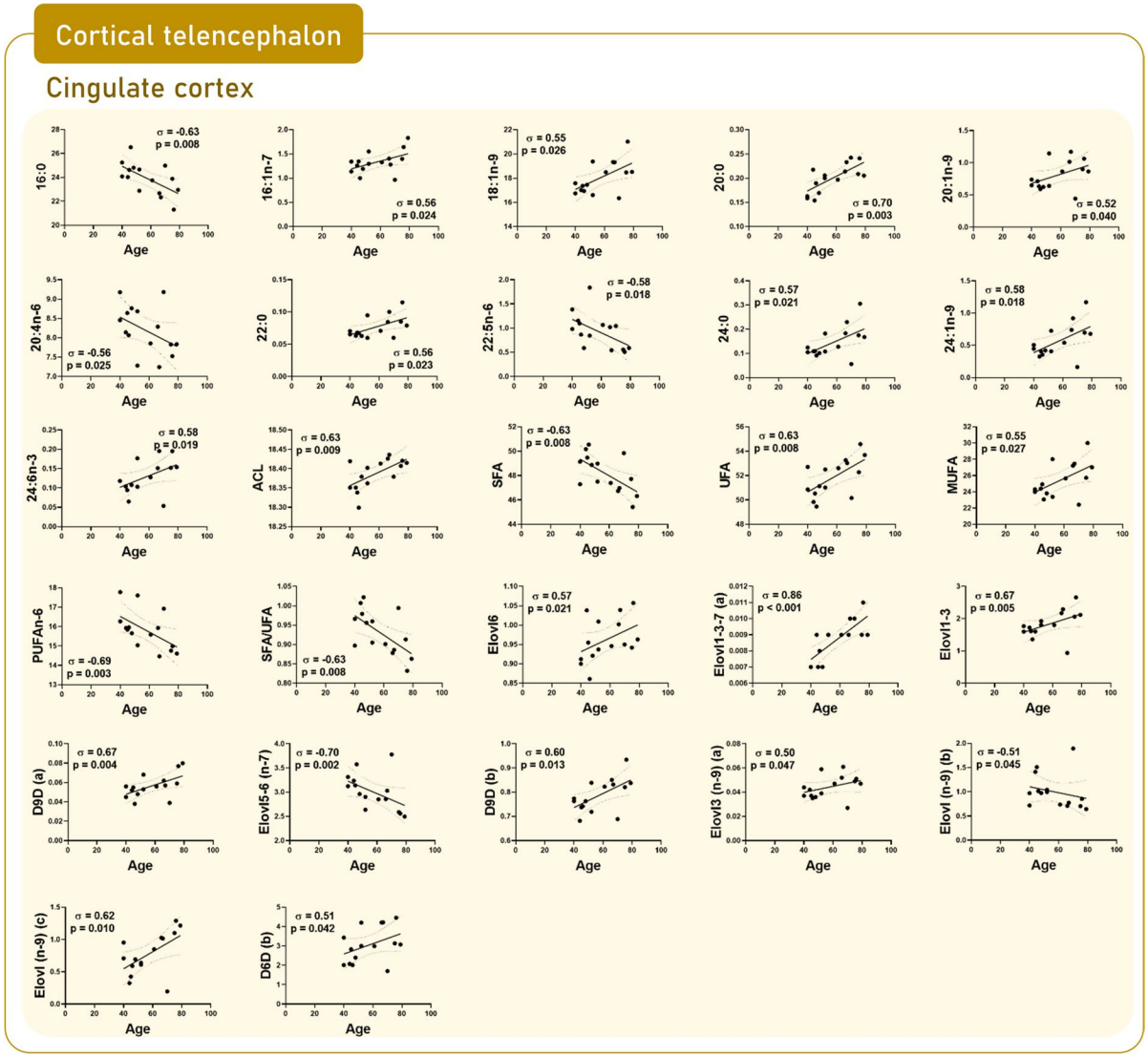

Fig. 6 Scatterplots by region based on significant correlations between fatty acids and calculated indexes and age in inferior temporal cortex (area 20)

attributed to an increase in D9D activity, the 20:4n-6 and 22:5n-6 decreases do not appear to depend on changes in the desaturase and elongase activity of their biosynthesis pathway, so the alteration in their content should be attributed to potential increases in its consumption [32], since they are fatty acids that act as substrates for the biosynthesis of eicosanoids and resolvins, respectively [9]. The consequences of these specific fatty acid profile changes are multiple. Thus, the changes in MUFAs and PUFAn-6 abundance can have repercussions at two levels: the first of them with implications in the geometric properties of lipids that can negatively affect functions such as exocytosis and formation of membrane microdomains [4]; and as to the second, the roles of affected PUFAn-6 are key in the generation of lipid mediators and, in particular, the synthesis of bioactive lipids with anti-inflammatory and neuroprotective properties that ensure cell survival and normal functioning during normal aging [9, 33]. Therefore, we hypothesize that the changes at the molecular and cellular levels described during human aging in the inferior

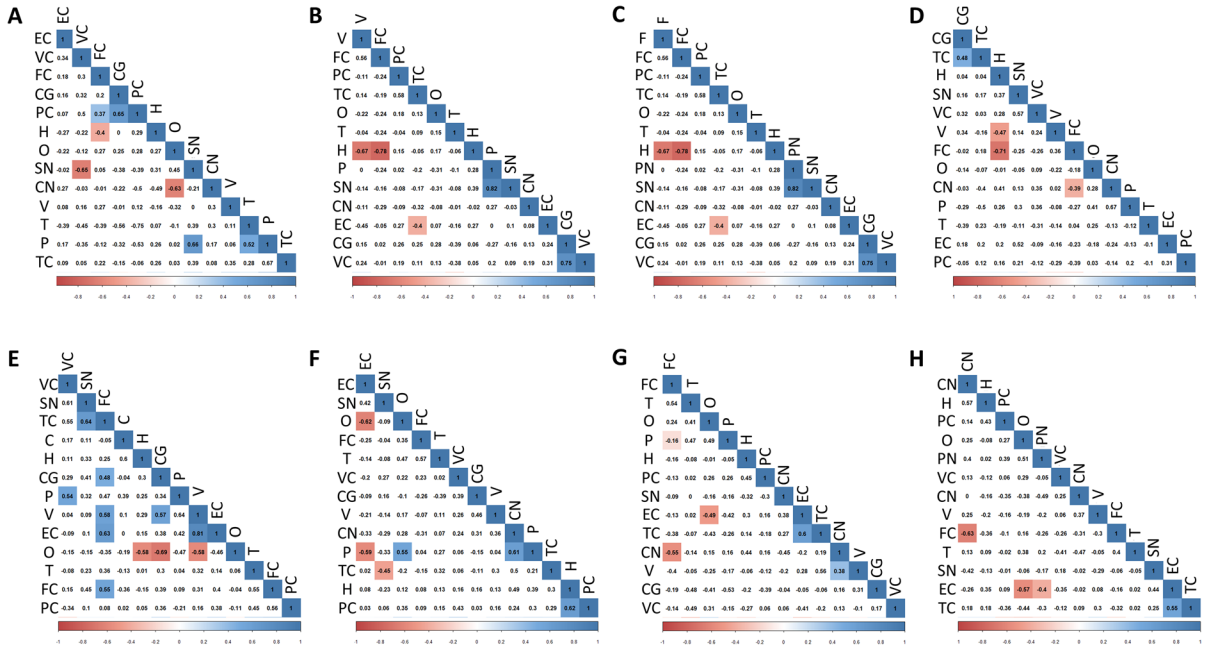

Fig. 7 Correlation matrix for integrative indexes calculated from fatty acid composition to evaluate the existence of regional relationships. **A** Average chain length (ACL); **B** saturated fatty acids (SFA); **C** Unsaturated fatty acids (UFA); **D** monounsaturated fatty acids (MUFA); **E** polyunsaturated fatty acids n-6 series (PUFAn6), **F** polyunsaturated fatty acids series n-3 (PUFAn3); **G** double bond index (DBI); **H** peroxidizability index (PI). Brain regions: CG, cingulate gyrus; CN, caudate nucleus; EC, entorhinal cortex; FC, frontal cortex; H, hippocampus; O, olive; P, putamen; PC, parietal cortex; SN, substantia nigra; T, thalamus; TC, temporal cortex; V, vermis; VC, visual (occipital) cortex

Table 3 Statistics of the FDR adjustment for multiple correlations

	Brain region	Variable	rho	*P* value (original)	*P* value at FDR 10%
Hindbrain	*Olive*	14:0	−0.801	0.001	0.001
	Vermis	20:0	0.745	0.001	0.035
Diencephalon	*Thalamus*	22:4n6	−0.862	0.001	0.001
		ACL	−0.823	0.001	0.001
Subcortical telencephalon	*Putamen*	22:4n6	−0.810	0.001	0.001
		ACL	−0.812	0.001	0.001
Cortical telencephalon	*Temporal cortex*	18:1n9	0.709	0.001	0.018
		22:4n6	−0.685	0.006	0.023
		PUFAn6	−0.708	0.001	0.018
	Cingulate cortex	16:0	−0.630	0.008	0.045
		20:0	0.700	0.003	0.045
		ACL	0.630	0.009	0.045
		SFA	−0.640	0.008	0.045
		UFA	0.640	0.008	0.045
		PUFAn6	−0.690	0.003	0.045
		SFA/UFA	−0.640	0.008	0.045

p value threshold at FDR 10%. *ACL*, average chain length; *SFA*, saturated fatty acids; *UFA*, unsaturated fatty acids; *PUFAn6*, polyunsaturated fatty acids series n6. Only significant differences are indicated. For more information, see Table S2

frontal cortex [34, 35] and cingulate cortex [36]—which can give rise to functional losses in high-level visual processing and recognition memory, as well as emotional regulation, attention, and the integration of emotional and cognitive processes, respectively—may have as a substrate, at least in part, the alterations of the lipid profile described in this study. However, the underlying molecular mechanisms that determine the high susceptibility of these brain areas to the aging process instead of other regions is a question that remains unknown and more studies are needed to clarify this finding.

In contrast to the compositional sustainability with aging that characterizes most brain areas, in pathological conditions such as Alzheimer's disease (AD) a marked change in temporal trajectory of the lipid profile is observed. Effectively, the involvement of lipid alterations in AD brains has been well-established in the last years, in particular with reference to PUFA and cholesterol contents (reviewed in [37–39]). Alterations of lipid profile affecting both gross brain lipids and lipid rafts were described in different brain regions affected by AD such as entorhinal cortex, hippocampus, and frontal cortex. In particular, it has been reported abnormally low levels of PUFAn-3 (mainly 22:6n-3) and monoenes, along with lower 20:4n-6 and cholesterol contents, among other lipidomic alterations [39, 40]. Importantly, these changes were exhibited at advanced stage of AD, but also in very early stages of the disease, suggesting that lipid alterations are early events in the pathogenesis of AD. Concomitantly, an increased level of lipoxidative damage specifically targeted to proteins involved in energy metabolism, cytoskeleton, neurotransmission, proteostasis, and oxygen metabolism has been described in AD [39]. Interestingly, these affected biological processes play a central role in the neuronal lost and subsequent functional decline associated with AD [39]. Thus, it can be hypothesized that a combination of increased oxidative stress, deficits in mitochondrial bioenergetics, and disruption of lipid homeostasis overcomes the ability to maintain lipid membrane composition, becoming a seminal condition during the development of the disease, in contrast to what occurs during normal brain aging.

Another interesting observation of the present study is that some of the observed changes in fatty acid profile with age showed a breakpoint after the age of 50. This finding is in line with additional changes such as transcriptional defects related to mitochondrial electron transport chain and signaling pathways involved in neuronal survival, decreased concentration of the main lipid classes, and increased oxidation-derived protein damage that also take place at this age [38, 41–43]. In this context, it is plausible to postulate that these adaptive changes might represent, when they reach a threshold value, the molecular substrate determining a bifurcation of the normal temporal trajectory toward the onset of AD pathology.

Globally, age-associated changes in terms of individual fatty acid content in the brain are heterogeneous. Thus, forebrain appears to be the region most affected by the aging process. Few changes were found in substantia nigra in the midbrain, whereas hindbrain global fatty acid composition appeared to be unaffected by the aging process. Our findings also suggest that major adult human brain fatty acids undergo slight but progressive and significant changes in their abundance during the aging process, with some changes showing a breakpoint after the age of 50. However, the individual contribution of these fatty acid patterns to the aging process is as yet unknown. Therefore, goals of future research are to define which types of lipid molecular species change with age in the different human brain regions, to extend the lipidomics analysis to additional brain regions not studied, to analyze lipid patterns according to neural cell-type specificity, and how they relate both to the function of the area and to the dysfunction leading to neuropathology. Indeed, it is not yet known whether the changes in fatty acids represent neutral changes with age, changes causing physiological aspects of aging, or adaptative responses to damaging agents. In any case, the findings described here suggest that fatty acids and their metabolism are closely linked to human brain aging.

Acknowledgements M.J. is a "Serra-Hunter" Fellow. We thank Alba Naudí and David Argiles for technical support. We thank T. Yohannan for editorial help.

Author contribution Conceptualization, M.J., I.F., and R.P.; methodology, M.J., I.F., and R.P.; software, N.M-M., M.J., J.S., and R.P.; formal analysis, N.M-M., P.A-B., M.M-G., J.D.G-L., J.S., and A.F-B.; investigation, M.P-O., M.J., and R.P.; resources, R.P.; data curation, N.M-M., J.S., M.J., M.P-O., and R.P.; writing, original draft preparation, M.J., I.F., and R.P.; writing, review and editing, M.J., I.F., and R.P.; visualization, M.J., and R.P.; supervision, M.J., and R.P.; project

administration, R.P.; funding acquisition, R.P. All authors have read and agreed upon the published version of the manuscript.

Funding Open Access funding provided thanks to the CRUE-CSIC agreement with Springer Nature. This research was funded by the Spanish Ministry of Science, Innovation, and Universities (grant RTI2018-099200-B-I00), the IRBLleida-Dipuatació de Lleida (PIRS2021), and the Generalitat of Catalonia: Agency for Management of University and Research Grants (2017SGR696) to R.P. This study was cofinanced by FEDER funds from the European Union ("A way to build Europe"). IRBLleida is a CERCA Programme/Generalitat of Catalonia.

Data availability The datasets generated and/or analyzed during the current study are available from the corresponding author upon reasonable request.

Declarations

Ethics approval The study was conducted according to the guidelines of the Declaration of Helsinki, the guidelines of Spanish legislation (Real Decreto 1716/2011), and the approval of the local ethics committee (CEIC/1981).

Informed consent Not applicable.

Conflict of interest The authors declare no competing interests.

References

1. Bozek K, Wei Y, Yan Z, Liu X, Xiong J, Sugimoto M, Tomita M, Pääbo S, Sherwood CC, Hof PR, Ely JJ, Li Y, Steinhauser D, Willmitzer L, Giavalisco P, Khaitovich P. Organization and evolution of brain lipidome revealed by large-scale analysis of human, chimpanzee, macaque, and mouse tissues. Neuron. 2015;85:695–702.
2. Crawford MA, Schmidt WF, Broadhurst CL, Wang Y. Lipids in the origin of intracellular detail and speciation in the Cambrian epoch and the significance of the last double bond of docosahexaenoic acid in cell signaling. Prostaglandins Leukot Essent Fatty Acids. 2021;166:102230.
3. Sastry PS. Lipids of nervous tissue: composition and metabolism. Prog Lipid Res. 1985;24:69–176.
4. Piomelli D, Astarita G, Rapaka R. A neuroscientist's guide to lipidomics. Nat Rev Neurosci. 2007;8:743–54.
5. Naudí A, Cabré R, Jové M, Ayala V, Gonzalo H, Portero-Otín M, Ferrer I, Pamplona R. Lipidomics of human brain aging and Alzheimer's disease pathology. Int Rev Neurobiol. 2015;122:133–89.
6. Yetukuri L, Ekroos K, Vidal-Puig A, Orešič M. Informatics and computational strategies for the study of lipids. Mol BioSyst. 2008;4:121–7.
7. Purdon AD, Rosenberger TA, Shetty HU, Rapoport SI. Energy consumption by phospholipid metabolism in mammalian brain. Neurochem Res. 2002;27:1641–7.
8. Hagen RM, Rodriguez-Cuenca S, Vidal-Puig A. An allostatic control of membrane lipid composition by SREBP1. FEBS Lett. 2010;584:2689–98.
9. Farooqui AA. Lipid mediators in the neural cell nucleus: their metabolism, signaling, and association with neurological disorders. Neuroscientist. 2009;15:392–407.
10. Naudí A, Cabré R, Dominguez-Gonzalez M, Ayala V, Jové M, Mota-Martorell N, Piñol-Ripoll G, Gil-Villar MP, Rué M, Portero-Otín M, Ferrer I, Pamplona R. Region-specific vulnerability to lipid peroxidation and evidence of neuronal mechanisms for polyunsaturated fatty acid biosynthesis in the healthy adult human central nervous system. Biochim Biophys Acta – Mol Cell Biol Lipids. 2017;1862:485–95.
11. Ferrer I, Martinez A, Boluda S, Parchi P, Barrachina M. Brain banks: benefits, limitations and cautions concerning the use of post-mortem brain tissue for molecular studies. Cell Tissue Bank. 2008;9:181–94.
12. Braak H, Thal DR, Ghebremedhin E, Del Tredici K. Stages of the pathologic process in Alzheimer disease: age categories from 1 to 100 years. J Neuropathol Exp Neurol. 2011;70:960–9.
13. Ferrer I. Defining Alzheimer as a common age-related neurodegenerative process not inevitably leading to dementia. Prog Neurobiol. 2012;97:38–51.
14. Jové M, Ayala V, Ramírez-Núñez O, Naudí A, Cabré R, Spickett CM, Portero-Otín M, Pamplona R. Specific lipidome signatures in central nervous system from methionine-restricted mice. J Proteome Res. 2013;12:2679–89.
15. Wei T, Simko V. R package "corrplot": Visualization of a Correlation Matrix (Version 0.88). Available from https://github.com/taiyun/corrplot. 2021.
16. Harrell FE Jr, Dupont C. Hmisc: Harrell Miscellaneous. R package version 4.5–0. https://CRAN.R-project.org/package=Hmisc. 2021.
17. Burger M. Seidel K [Chemical biomorphosis of the human brain and sciatic nerve; a survey]. Z Alternsforsch. 1958;12:52–79.
18. Rouser G, Yamamoto A. Curvilinear regression course of human brain lipid composition changes with age. Lipids. 1968;3:284–7.
19. Ledesma MD, Martin MG, Dotti CG. Lipid changes in the aged brain: effect on synaptic function and neuronal survival. Prog Lipid Res. 2012;51:23–35.

20. Farooqui AA, Liss L, Horrocks LA. Neurochemical aspects of Alzheimer's disease: involvement of membrane phospholipids. Metab Brain Dis. 1988;3:19–35.
21. Söderberg M, Edlund C, Kristensson K, Dallner G. Lipid compositions of different regions of the human brain during aging. J Neurochem. 1990;54:415–23.
22. Horrocks LA, Van Rollings M, Yates AJ. Lipid changes in the ageing brain. In The Molecular Basis of Neuropathology, Davinson AN, Thompson RHS, Eds. Edward Arnold: London, United Kingdom, 1981.
23. Svennerholm L, Boström K, Helander CG, Jungbjer B. Membrane lipids in the aging human brain. J Neurochem. 1991;56:2051–9.
24. Svennerholm L, Boström K, Jungbjer B, Olsson L. Membrane lipids of adult human brain: lipid composition of frontal and temporal lobe in subjects of age 20 to 100 years. J Neurochem. 1994;63:1802–11.
25. Hancock SE, Friedrich MG, Mitchell TW, Truscott RJW, Else PL. Decreases in phospholipids containing adrenic and arachidonic acids occur in the human hippocampus over the adult lifespan. Lipids. 2015;50:861–72.
26. Norris SE, Friedrich MG, Mitchell TW, Truscott RJW, Else PL. Human prefrontal cortex phospholipids containing docosahexaenoic acid increase during normal adult aging, whereas those containing arachidonic acid decrease. Neurobiol Aging. 2015;36:1659–69.
27. Hancock SE, Friedrich MG, Mitchell TW, Truscott RJ, Else PL. The phospholipid composition of the human entorhinal cortex remains relatively stable over 80 years of adult aging. Geroscience. 2017;39:73–82.
28. Martín V, Fabelo N, Santpere G, Puig B, Marín R, Ferrer I, Diaz M. Lipid alterations in lipid rafts from Alzheimer's disease human brain cortex. J Alzheimers Dis. 2010;19:489–502.
29. Carver JD, Benford VJ, Han B, Cantor AB. The relationship between age and the fatty acid composition of cerebral cortex and erythrocytes in human subjects. Brain Res Bull. 2001;56:79–85.
30. Cabré R, Naudí A, Dominguez-Gonzalez M, Jové M, Ayala V, Mota-Martorell N, Pradas I, Nogueras L, Rué M, Portero-Otín M, Ferrer I, Pamplona R. Lipid profile in human frontal cortex is sustained throughout healthy adult life span to decay at advanced ages. J Gerontol A Biol Sci Med Sci. 2018;73:703–10.
31. McNamara RK, Liu Y, Jandacek R, Rider T, Tso P. The aging human orbitofrontal cortex: decreasing polyunsaturated fatty acid composition and associated increases in lipogenic gene expression and stearoyl-CoA desaturase activity. Prostaglandins Leukot Essent Fatty Acids. 2008;78:293–304.
32. Domínguez-González M, Puigpinós M, Jové M, Naudi A, Portero-Otín M, Pamplona R, Ferrer I. Regional vulnerability to lipoxidative damage and inflammation in normal human brain aging. Exp Gerontol. 2018;111:218–28.
33. Das UN. Ageing: Is there a role for arachidonic acid and other bioactive lipids? A review J Adv Res. 2018;11:67–79.
34. Scheff SW, Price DA, Schmitt FA, Scheff MA, Mufson EJ. Synaptic loss in the inferior temporal gyrus in mild cognitive impairment and Alzheimer's disease. J Alzheimers Dis. 2011;24:547–57.
35. Xu B, Xiong F, Tian R, Zhan S, Gao Y, Qiu W, Wang R, Ge W, Ma C. Temporal lobe in human aging: A quantitative protein profiling study of samples from Chinese Human Brain Bank. Exp Gerontol. 2016;73:31–41.
36. Mann SL, Hazlett EA, Byne W, Hof PR, Buchsbaum MS, Cohen BH, Goldstein KE, Haznedar MM, Mitsis EM, Siever LJ, Chu KW. Anterior and posterior cingulate cortex volume in healthy adults: effects of aging and gender differences. Brain Res. 2011;1401:18–29.
37. Jové M, Portero-Otín M, Naudí A, Ferrer I, Pamplona R. Metabolomics of human brain aging and age-related neurodegenerative diseases. J Neuropathol Exp Neurol. 2014;73:640–57.
38. Naudí A, Cabré R, Jové M, Ayala V, Gonzalo H, Portero-Otín M, Ferrer I, Pamplona R. Lipidomics of human brain aging and Alzheimer's disease pathology. Int Rev Neurobiol. 2015;122:133–89.
39. Jové M, Mota-Martorell N, Torres P, Ayala V, Portero-Otin M, Ferrer I, Pamplona R. The causal role of lipoxidative damage in mitochondrial bioenergetic dysfunction linked to Alzheimer's Disease pathology. Life (Basel). 2021;11:388.
40. Fabelo N, Martín V, Marín R, Moreno D, Ferrer I, Díaz M. Altered lipid composition in cortical lipid rafts occurs at early stages of sporadic Alzheimer's disease and facilitates APP/BACE1 interactions. Neurobiol Aging. 2014;35:1801–12.
41. Cabré R, Naudí A, Dominguez-Gonzalez M, Ayala V, Jové M, Mota-Martorell N, Piñol-Ripoll G, Gil-Villar MP, Rué M, Portero-Otín M, Ferrer I, Pamplona R. Sixty years old is the breakpoint of human frontal cortex aging. Free Radic Biol Med. 2017;103:14–22.
42. Lu T, Aron L, Zullo J, Pan Y, Kim H, Chen Y, Yang TH, Kim HM, Drake D, Liu XS, Bennett DA, Colaiácovo MP, Yankner BA. REST and stress resistance in ageing and Alzheimer's disease. Nature. 2014;507:448–54.
43. Aron L, Zullo J, Yankner BA. The adaptive aging brain. Curr Opin Neurobiol. 2021;72:91–100.